INSTITUTO POLITÉCNICO DE BRAGANÇA
Escola Superior de Tecnologia e de Gestão

VALORIZATION OF WASTE COOKING OILS THROUGH CONVERSION PROCESSES CATALYSED BY CHOLINE HYDROXIDE

Yara Dos Ramos Gué

Dissertation presented to the *Escola Superior de Tecnologia e Gestão* of the *Instituto Politécnico de Bragança* to the fulfilment of requirements to obtain the Master Degree in Chemical Engineering

Supervisors

Prof. Dra. Ana Queiroz

Prof. Dr. António Ribeiro

Prof. Dr. Paulo Brito

BRAGANÇA 2021

“Nossa maior fraqueza está em desistir. A maneira certa de ter sucesso é tentar apenas mais uma vez.”

Thomas Edison

ACKNOWLEDGEMENTS

It would not have been possible to write this master´s thesis without the help and support of the kind people around me, just a few of whom it is possible to give mention here.

I would like to thank the supervisors Professor Ana Queiroz, Professor Paulo Brito, and Professor António Ribeiro, for the opportunity to carry out this work under your guidance and for all the help needed along this path, contributing to my personal enrichment and growth.

I also thank Dr. Paula Plasencia and Engineer Maria João Afonso for their laboratory support.

To my mother, Nira, my father Arlindo my brother Yuri and Arlito, I must thank for everything I've achieved, for all your support, trust, affection, and love, without you none of this would be possible.

To my laboratory colleagues Fretson Almeida and Fábio Monteiro, thank you for the company and shared teachings.

I am eternally grateful to my family, my friends who always always supported me and believed that all this would be possible.

ABSTRACT

Biodiesel is a biofuel produced from renewable biomass through the reaction of transesterification of triglycerides through an alcohol in the presence of a catalyst. Interest in this fuel is related to the search for alternatives to petroleum-based energy sources. This is associated with several environmental benefits, such as a reduction in the emission of pollutants. However, due to the high cost associated with its usual raw material, such as edible vegetable oils, biodiesel is currently not economically viable. Therefore, it is necessary to reduce the final price of this fuel. One of the ways to reduce costs will be the use of cheaper raw materials in the production process, such as used oils or non-edible ones. One of the main features of these cheaper raw materials is their low quality compared to edible oils. This low quality is associated with a high content of free fatty acids (FFA) and/or water. The FFAs present in the raw material must be converted into biodiesel, also known as fatty acid metal esters (Fatty Acid Methyl Esters: FAME) by a transesterification reaction.

In the present study, the use of the choline hydroxide catalyst in the production of biodiesel through the transesterification reaction, in a waste cooking oil (WCO) with acidity manipulation, is evaluated. The influence of the main operation parameters: temperature, molar ratio WCO/methanol, catalyst dosage and oleic acid (OA) incorporation for control of acidity, was studied using a response surface methodology based in a Box-Behnken Design (BBD), evaluating two main responses: FAME content and the yield of the reaction.

The most relevant factors were the molar ratio between waste cooking oil and methanol, catalyst dosage and incorporation of oleic acid. For main responses: FAME content and yield. It was possible to define the ideal conditions that lead to the greatest possible FAME content and the highest possible yield. The optimal condition to obtain 85.4% FAME content and 73.7% of yield was estimated at 63ºC, molar ratio of 1:13, 1.5wt% of catalyst and 0.5wt% of OA incorporation.

Keywords: Biodiesel production; Transesterification; Ionic liquids; Choline Hydroxide; Response surface methodology.

RESUMO

O biodiesel é um biocombustível produzido a partir de biomassa renovável por meio da reação de transesterificação de triglicerídeos na presença de um álcool e de um catalisador. O interesse por esse combustível está relacionado à busca de alternativas às fontes de energia derivadas do petróleo. Isso está associado a diversos benefícios ambientais, como a redução na emissão de poluentes. Porém, devido ao alto custo associado à sua matéria-prima usual, como os óleos vegetais comestíveis, o biodiesel atualmente não é viável economicamente. Portanto, é necessário reduzir o preço final desse combustível. Uma das formas de reduzir custos será a utilização de matérias-primas mais baratas no processo produtivo, como óleos usados ou não comestíveis. Uma das principais características dessas matérias-primas mais baratas é a baixa qualidade em relação aos óleos comestíveis. Essa baixa qualidade está associada a um alto teor de ácidos graxos livres (FFA) e / ou água. Os FFAs presentes na matéria-prima devem ser convertidos em biodiesel, também conhecidos como ésteres metálicos de ácidos graxos (Ésteres Metílicos de Ácidos Gordos: FAME) por meio de uma reação de transesterificação.

No presente estudo, é avaliada a utilização do catalisador hidróxido de colina na produção de biodiesel por meio da reação de transesterificação num óleo alimentar residual (WCO) com manipulação de acidez. A influência dos parâmetros de operação principais: temperatura, razão molar WCO/metanol, dosagem de catalisador e incorporação de ácido oleico (OA) para alteração de acidez, foi estudada usando uma metodologia de superfície de resposta baseada num Box-Behnken Design (BBD), avaliando duas respostas principais: o teor de FAME e o rendimento da reação.

Os fatores mais relevantes foram a relação molar entre óleo de cozinha residual e metanol, a dosagem do catalisador e a incorporação de ácido oleico. Para as principais respostas: Conteúdo FAME e o rendimento. Foi possível definir as condições ideais que levaram ao maior conteúdo de FAME possível e ao maior rendimento possível. A condições ótimas para a obtenção de 88,2% de teor de FAME e 64,8% do rendimento foi estimada à 58 ° C, razão molar de 1:15, 2wt% de catalisador e 0,5wt% de incorporação do OA.

Palavras-chave: Produção de biodiesel; Transesterificação; Hidróxido de colina; Líquidos iónicos; Metodologia de superfície e respostas.

TABLE OF CONTENTS

ABSTRACT iii

RESUMO iv

LIST OF FIGURES vii

LIST OF TABLES x

NOMENCLATURE xi

1. BACKGROUND AND OBJECTIVES 1

1.1 BACKGROUND 1

1.2 OBJECTIVES 2

1.3 REPORT STRUCTURE 2

2. BIODIESEL 3

2.1 ADVANTAGES AND DISADVANTAGES 4

2.2 PRODUCTION 4

2.2.1 First Generation 5

2.2.2 Second and Third Generation 5

2.3 FEEDSTOCKS 7

2.4 METHODS OF PRODUCTION 9

2.4.1 Esterification 9

2.4.2 Transesterification 10

2.5 CATALYSTS 12

2.6 PHYSICO-CHEMICAL CHARACTERIZATION 15

3. IONIC LIQUIDS 18

3.1 IONIC LIQUIDS IN BIODIESEL PRODUCTION 19

3.2 LITERATURE REVIEW 20

3.3 CHOLINE HYDROXIDE 23

3.3.1 CHOLINE HYDROXYDE SYNTHESIS 24

3.4 REVIEW OF PREVIOUS WORKS 25

4. TECHNICAL DESCRIPTION AND PROCEDURES 29

4.1 REAGENTS AND RAW MATERIALS 29

4.2 EQUIPMENT 29

4.3 METHODOLOGY 30

4.3.1 Transesterification Reaction of waste cooking oil 30

4.3.2 FAME content by Gas Chromatography 32

4.4 VOLUMETRIC MEASUREMENTS 36

4.4.1 Acidity Measurement 36

4.4.2 Determination of basicity of choline hydroxide solution in methanol 36

4.5 DERIVATIZATION OF FATTY ACIDS BY BF_3 37

4.6 FTIR ANALYSIS 38

4.7 EXPERIMENTAL DESIGN 39

5. RESULTS AND DISCUSSION 41

5.1 FEEDSTOCK CHARACTERIZATION 41

5.2 CHOLINE HYDROXIDE 45

5.3 EXPERIMENTAL DESIGN 47

5.3.1 Analyses for the acidity value response 49

5.3.2 Analyses for FAME content 59

6. CONCLUSIONS AND SUGGESTIONS OF FUTURE WORK 75

7. REFERENCES 77

LIST OF FIGURES

Figure 1. Potential dominant first-generation biodiesel feedstock of each country 9
Figure 2. General Esterification mechanism. 10
Figure 3. Transesterification mechanism..... 11
Figure 4. Structure of choline hydroxide. 23
Figure 5. Synthesis of choline hydroxide using choline chloride and potassium hydroxide. 24
Figure 6. Experimental apparatus for the transesterification reaction to produce biodiesel. 30
Figure 7. Phase separation; Phase (1): organic or biodiesel phase. Phase (2): glycerol + catalyst phase. 31
Figure 8. Phase separations in 15 mL flasks; (1): Light phase, (2): Heavy phase. 31
Figure 9. GC-FID equipment used for FAME content analysis in biodiesel samples. .. 32
Figure 10. Chromatographic analysis obtained for the Supelco 37 Component FAME. Mix on the Omegawax 250 column. 33
Figure 11. Perking Elmer FTIR, Spectrum Two model. 39
Figure 12. Chromatograms obtained by GC-FID for samples of oleic acid after derivatization. 42
Figure 13. Chromatograms obtained by GC-FID for samples of waste cooking oil after derivatization. 43
Figure 14. FTIR spectrum of oleic acid. 44
Figure 15. FTIR spectrum of waste cooking oil. 45
Figure 16. FTIR spectrum of choline hydroxide solution, 45 wt.% in methanol. 46
Figure 17. Normal plot of residuals for the acidity value (**A**); Residual versus predicted for the acidity value(**B**). 51
Figure 18. Response surface regarding the influence of temperature (A) and molar ratio WCO/methanol (B) on the acidity value and the interaction plot of those variables. 52
Figure 19. Response surface regarding the influence of temperature (A) and catalyst dosage (C) on the acidity value and the interaction plot of those variables. 53
Figure 20. Response surface regarding the influence of temperature (A) and incorporation of oleic acid (D) on the acidity value and the interaction plot of those variables. 54
Figure 21. Response surface regarding the influence of molar ratio WCO/MeOH (B) and catalyst dosage (C) on the acidity value and the interaction plot of those variables. 55

Figure 22. Response surface regarding the influence of molar ratio WCO/MeOH (B) and incorporation of oleic acid (D) on the acidity value and the interaction plot of those variables. 56
Figure 23. Response surface regarding the influence of catalyst dosage (C) and incorporation of oleic acid (D) on the acidity value and the interaction plot of those variables (A= 0; B = 0). 57
Figure 24. Normal plot of residuals for the FAME content (**A**); Residual versus predicted for the FAME content (**B**). 61
Figure 25. Response surface regarding the influence of temperature (A) and molar ratio WCO/MeOH (B) on the FAME content and the interaction plot of those variables. 61
Figure 26. Response surface regarding the influence of temperature (A) and catalyst dosage (C) on the FAME content and the interaction plot of those variables. 62
Figure 27. Response surface regarding the influence of temperature (A) and incorporation of oleic acid (D) on the FAME content and the interaction plot of those variables. 63
Figure 28. Response surface regarding the influence of molar ratio WCO/MeOH (B) and catalyst dosage (C) on the FAME content and the interaction plot of those variables... 64
Figure 29. Response surface regarding the influence of molar ratio WCO/MeOH (B) and incorporation of oleic acid (D) on the FAME content and the interaction plot of those variables. 65
Figure 30. Response surface regarding the influence of catalyst dosage (C) and incorporation of oleic acid (D) on the FAME content and the interaction plot of those variables. 66
Figure 31. A: Normal plot of residuals for the yield; B: Residual versus predicted for the yield. 69
Figure 32. Response surface regarding the influence of temperature (A) and molar ratio WCO/MeOH (B) on the yield and the interaction plot of those variables. 69
Figure 33. Response surface regarding the influence of temperature (A) and catalyst dosage (C) on the yield and the interaction plot of those variables. 70
Figure 34. Response surface regarding the influence of temperature (A) and incorporation of oleic acid (D) on the yield and the interaction plot of those variables. 71
Figure 35. Response surface regarding the influence of molar ratio WCO/MeOH (B) and catalyst dosage (C) on the yield and the interaction plot of those variables. 72
Figure 36. Response surface regarding the influence of molar ratio WCO/MeOH (B) and incorporation of oleic acid (D) on the yield and the interaction plot of those variables. 72

Figure 37. Response surface regarding the influence of catalyst dosage (C) and incorporation of oleic acid (D) on the Yield and the interaction plot of those variables. 73

LIST OF TABLES

Table 1. Advantages and challenges of first, second and third generation biodiesel sources. 6
Table 2. Classification of some of the main feedstocks for biodiesel production. 8
Table 3. Types of catalysts employed in biodiesel production. 14
Table 4. Fatty acid profile of different feedstocks. 17
Table 5. Some experimental conditions found in the literature for biodiesel production. 22
Table 6. Summary of preview works done by the research group. 28
Table 7. Elution order, compound name, compound ID and retention time for the 37 compounds. 35
Table 8. Experimental information of independent variables in BBD 39
Table 9. Experimental conditions applied for each run, in coded and in real values. 40
Table 10. Acidity values of raw materials. 41
Table 11. FAME profile obtained after derivatization of oleic acid. 42
Table 12. FAME profile obtained after derivatization of waste cooking oil. 43
Table 13. Titration of ChOH(CH3OH) solution 46
Table 14. Experimental design, real conditions, and experimental responses. 48
Table 15. ANOVA analysis for the parameters influencing the acidity value. 50
Table 16. Coefficients for acidity value. 58
Table 17. Optimal conditions for acidity value. 58
Table 18. Analysis of variance for the fitted quadratic model for FAME content. 60
Table 19. Coefficients for FAME content. 67
Table 20. Best conditions for FAME content. 67
Table 21. Analysis of variance for the fitted quadratic model for yield. 68
Table 22. Coefficients for yield. 74
Table 23. Best conditions for yield. 74

NOMENCLATURE

Acronyms and Symbols

wt	Weight
AV	Acid Value
B100	Pure Biodiesel
b.p	Boiling Point
CN	Cetane Number
OA	Oleic Acid
SFO	Sunflower Oil
TAG	Triacylglycerol
DES	Deep Eutetic Solvent
EED	Eletro-Eletrodialysis
UCO	Used Cooking Oil
WCO	Waste Cooking Oil
WFO	Waste Frying Oil
EN	European Standard
EU	European Union
FFA	Free Fatty Acids
GC	Gas chromatography
GHG	Greenhouse Gas
CC	Cooking Oil
GL	Glycerol
IL	Ionic Liquid
LCA	Life Cycle Analysis
FAAE	Fatty Acid Alkyl Esters
FAME	Fatty Acid Methyl Esters
DTA	Differential Thermal Analyzer
EDX	Energy Dispersive X-Ray
TGA	Themo Gravimetric Analyzer
TSIL	Task-Specific Ionic Liquids
XRD	X-Ray Diffraction Analyzer
BBD	Box-Behnken Design
SEM	Scanning Electron Microscopy

NMR	Nuclear Magnetic Resonance
RSM	Response Surface Methodology
B20	Fuel with 20% concentration in biodiesel
BET	Brunauer-Emmett-Feller Spectroscopy
ASTM	American Society for Testing and Materials (ASTM International)
CO_2-TPD	Temperature- Programmed Desorption of Carbon Dioxide
GC-FID	Gas Chromatograph with flame ionization detector
FTIR	Fourier Transform Infrared Spectroscopy

Formulas

[BMIM][$MeSO_4$]	1-butyl-3-methyl imidazolium methyl sulfate
[BIM][HSO_4]	Butylimidazolium hydrogen sulfate
[BMIM]Br	1-Butyl-3-methylimidazolium bromide
[BMIM]HSO_4	1-Butyl-3-methylimidazolium hydrogen sulfate
[BMIM][CH_3SO_3]	1-Butyl-3-methylimidazolium methanesulfonate
[BMIM][CH_3SO_4]	1-Butyl-3-methylimidazolium methylsulfate
[MIM]HSO_4	Methylimidazolium hydrogen sulfate
BNPs-CCH	CCH stabilized on boehmite nanoparticles
CaO	Calcium oxide
CC	Choline Chloride
CCH	Chlorocholine hydroxide
CFA/Z_nO	Fly ash compound of zinc carbon-oxide
CH_3OH	Methanol
CH_3ON_a	Sodium methanolate
ChIm	Choline imidazolium
ChOH	Choline hydroxide
ChOMe	Choline methoxide
HCl	Hydrochloric acid
H_3PO_4	Phosphoric acid
H_2SO_4	Sulfuric acid
KOH	Potassium hydroxide
MeOH	Methanol
NaOH	Sodium hydroxide
NO_x	Nitrogen oxides
SOx	Sulfur oxides
Z_nMA	Zinc methacrylate
Z_nO	Zinc oxide

1. BACKGROUND AND OBJECTIVES

1.1 BACKGROUND

The world is facing great challenges due to the reduction of unrecoverable fossil fuels, the dependence on its industry, the increase in energy consumption and the increase in environmental pollution. A large amount of energy needs across the world is met by fossil fuels (petrochemical, coal, and natural gas) [1, 2].

The development of renewable energy resources is necessary to create the need for other alternatives to fossil fuels [3, 4, 5]. Biodiesel, as a renewable energy resource, is used as an alternative fuel in diesel engines [2, 6].It is known as one of the most promising renewable fuels for its biodegradability and sustainability [7]. Biodiesel can be defined as mono-alkyl esters of long-chain fatty acids produced from vegetable or animal oils and alcohol with or without a catalyst. It can be produced by esterification of fatty acids or transesterification of triglycerides with short chain alcohols, such as methanol and ethanol. Methanol is used mainly due to its lower cost compared with other alcohols, so biodiesel most commonly refers to fatty acid methyl esters (FAME) [1, 3, 8].

The use of biodiesel could reduce the emission of exhaust greenhouse gases, unburned hydrocarbons, particulate matters, poly-aromatics, and sulfur from the engines. The raw material are obtained from edible and non-edible oil sources including palm oil, jatropha oil, mustard oil, beauty leaf oil, microalgae oil, rubber seed oil, mahua oil, animal fats, waste cooking oil, can be used for biodiesel synthesis [1, 3].

Ionic liquids were initially introduced as alternative green reaction media due to their unique physicochemical properties such as non-volatility, non-flammability, thermal stability, and controlled miscibility. At present, these are extensively used in controlling the reaction as catalysts. Synthesis of biodiesel using ILs as a catalyst is a promising pathway to an eco-friendly production [1].

1.2 OBJECTIVES

The main objectives of this work are the optimization of operational parameters for the transesterification reaction using residual oil as raw material and choline hydroxide as catalyst, and the study of the catalyst recovery between several reaction cycles.

The most specific objectives are:

- ✓ Analysis of the transesterification in relation to FAME (Fatty Acid Methyl Esters) production, from waste cooking oil, using the alkaline catalyst: choline hydroxide.
- ✓ Optimization of reaction parameters: temperature, percentage of catalyst, and molar ratio oil/methanol, with a fixed time.

1.3 REPORT STRUCTURE

Chapter 1 of this thesis presents a background and objectives, Chapter 2 is an introduction to biodiesel as a renewable source and its properties, Chapter 3 is production processes and literature review with information about, ChOH, ionic liquids and its types and properties. Chapter 4 gives a description of the experimental protocols developed and implemented and Chapter 5 that presents the results and discussion of the work. Finally, in Chapter 6 there are presented the main conclusions and suggestions for future work.

2. BIODIESEL

Biodiesel is a long chain ester of (C14–C24) and is synthesized from several lipid content sources including vegetable oils, animal fats and waste oil. Glycerol is a by-product of the biodiesel production process, and its productions is estimated to enhance the financial benefits of the biodiesel industry further. It has been reported that about 10 wt.% glycerol can be obtained from the total production volume, and it can be used as a combustion improver of diesel/biodiesel. Biodiesel shows similar characteristics to the diesel fuel in terms of beneficial physical and chemical properties, including viscosity, flash point and cetane number [7].

Biodiesel is a biofuel made from renewable biomass for use in engines and can partially or totally replace fossil fuels, such as diesel. Biodiesel or alkyl fatty acid ester can be produced from the transesterification reaction of triglycerides using an alcohol in the presence of a catalyst. Due to the reversibility of the reaction, an excess of alcohol is used to alter the balance on the side of the products. Several species of vegetable oils and animal fats, such as soy, canola, castor, cotton, beef tallow, in addition to residual oil can be used as raw material in the production of biodiesel. The biodiesel produced in the industry is obtained by the homogeneous reaction of transesterification of triglycerides by means of basic catalysts, such as sodium and potassium hydroxides, carbonates and alkoxides. However, in the conventional industrial process, removal of the catalyst is technically difficult, and a large amount of wastewater is produced to separate and clean the catalyst and the product [2, 9].

This current study focused on the use of waste cooking oil (WCO) to produce biodiesel. The processing of WCO waste facilitates a consistent supply of raw material compared to competition with edible raw materials, which are more valuable as part of consumable food items. Thus, the use of WCO as a low-grade raw material for the synthesis of renewable fuel ensures price stability and process sustainability. The recycling of WCO prevents the accumulation of waste in the drainage system and reduces the cost of producing biodiesel. Furthermore, WCO is available in large quantities. Its management constitutes a serious disposal problem because it contaminates bodies of water and results in pipe clogging, damaging the maintenance economy of many nations. To curb these threats, spent cooking oil from different locations could be sent to a single collection unit and reused as a raw material to produce biodiesel [10].

2.1 ADVANTAGES AND DISADVANTAGES

Biofuels have several advantages such as cost efficiency, renewable energy source, reduced greenhouse gas emissions, reduced pollution, and economic stability for the country. As biofuels are cleaner fuels as opposed to fossil fuels, they increase the efficiency of the vehicle engine, thus increasing its useful life. In addition, biofuels rely on biomass as a source of production, making it an effective renewable energy option to overcome the energy crisis. Further, the scientists found that the use of biofuels reduces the emission of greenhouse gases by 65%, providing an alternative energy source in addition to fossil fuels. Price fluctuation has been a controversial issue in recent decades, which depends on the production of fossil fuels and the country's energy dependence, causing rapid instability in the global economy. It is assumed that the development of biofuels will change the prevailing condition to a more stable form. The effective way to sustain biodiesel productivity is to reduce dependence on edible raw materials and oil. Despite the numerous advantages, there are certain controversies associated with the production of biofuels. As the initial costs of producing this fuel are higher, an increase in energy demand in the future may affect energy production due to its higher production rate. In addition, the cultivation of biomass for biofuels can result in monoculture, which causes deficits in soil nutrients, making it inefficient for other crop varieties. Water pollution from the use of fertilizers for agricultural production and pollution from the biofuel industry were also identified as a negative influence. Without being overwhelmed by these disadvantages, scientists are working towards a sustainable strategy to provide energy sources without depleting biomass and providing a stable option to resolve the energy crisis [11, 12].

2.2 PRODUCTION

Depending on their source of production, biofuels are classified into three generations, first, second and third generation based on the chemical and complex nature of the biomass [12, 7]. The first-generation fuels, biodiesel and vegetable oils has been produced from the crop plants and the second, bioethanol and biohydrogen has been produced from agricultural by-products and energy plants which requires fertile lands for growth. The marine resources, seaweeds and cyanobacteria are attractive sources for the third-generation biofuels production (biogas, bioethanol and biobutanol) as they produce large biomass in a stipulated time period, and it doesn’t require land for growth [11].

2.2.1 First Generation

First generation biodiesel feedstocks are derived from food and edible oils. Commonly used feedstocks for first generation biodiesel include soybean, sunflower, oil palm, rapeseed, canola, and cottonseed. However, it has been argued that the use of edible food crops to produce first-generation biofuels effectively reduces the amount of edible food for human consumption, thus increasing food prices in the global food market. Although first generation biofuels help satisfy the human need for fuel, at the same time it depletes some resources intended for the even more important human need for nourishment [7].

2.2.2 Second and Third Generation

Second generation biodiesel is obtained from feedstocks from non-edible sources, e.g., crops, non-edible oil, and other non-edible sources such as wood, husk, which are then processed to produce biodiesel. These sources practically eliminate the dependency on edible food crops to produce fuel, which sparked the "food vs fuel" debate in the first place. Feedstocks used to produce second-generation biodiesel include *jatropha,* mahua, jojoba oil, tobacco seed, *Calophyllum,* and sea mango. Commercial and residential wastes are also included in this category. The use of these feedstocks to produce second generation biodiesel has been proven to be more efficient and more environmentally friendly compared to the feedstocks used for first generation biodiesel. However, some problems remain. By its very nature, crops require fertile land to grow, and the cultivation of non-edible crops for second generation biodiesel requires an extensive amount of fertile land, which competes with land used for the cultivation of edible food crops [7].

Third-generation biodiesel reduces both the food and land problems related to first- and second-generation biodiesel. Algae, specifically microalgae, are used as feedstocks to produce third generation biodiesel. The use of microalgae for biodiesel production is considered a more feasible alternative compared to feedstocks used for first and second-generation biodiesel, with microalgae having the potential to produce a yield of 15–300 times more than the yield from a traditional crop in relation to plantation area [7].

Table 1 shows the advantages and challenges of first, second and third generation biodiesel sources.

Table 1. Advantages and challenges of first, second and third generation biodiesel sources.

Biodiesel types	Sources	Advantages	Challenges
First generation	Edible oil feedstock	Renewable source	Competes with food crops (food-energy conflict)
		Environment-friendly	Rising cost of food due to food competition
		Easy conversion into biofuel	Land scarcity
Second generation	Non-edible oil feedstock	Renewable source	Land and water use competition
		Environment-friendly	Requires sophisticated down-stream processing technologies
		Does not compete with food crops	High production cost
		Effective land uti-lization (non-ara-ble lands)	Uncertain long-term supply of oil yield
Third generation	Oleaginous microbes	Renewable source	Insufficient biomass production for commercialization
		Environment-friendly	
		No conflict with food or land usage	
		Higher growth rate tendencies	High initial production and setup costs for economic viability (Large scale).
		High cell lipid ac-cumulation	

Source: Adapted from Mofijur *et al*., (2020) [7].

2.3 FEEDSTOCKS

To produce biodiesel, there are many raw materials available, namely edible and non-edible oils. The geographic distribution and the price of the raw material are the main factors to be considered in its selection.

Plant-derived oils are considered the most efficient raw materials due to its inexhaustible, biodegradable, non-toxic, renewable, and ecological nature. Based on regional soil fertility and environmental conditions, the availability of these oils differs significantly in several countries. Numerous edible oils have been investigated by several researchers as potential raw material [13].

The initial process of biodiesel production starts with the selection of feedstock which comprises mainly vegetable oils, animal fats, microbial oils, microalgae oils, and waste oils (like waste frying oil). Worldwide, there are more than 350 oil-bearing seeds which are prospective sources for biodiesel synthesis. The use of oils extracted from agricultural residues (crop residues, wood residues, etc.) to produce biodiesel could reduce the price of the raw material and avoid direct competition with the food industry [1, 14]. Some of the main feedstocks for biodiesel production are summarized in the Table 2.

Table 2. Classification of some of the main feedstocks for biodiesel production.

Vegetable oils		**Animal Fats**	**Microbial feedstocks**	**Waste oils**
Edible oils	**Nonedible oils**			
Soybeans (Glycine max)	Passion seed *(Passiflora edulis)*	Beef tallow	Fungi	Waste frying oil
Sunflower	Karanja or honge (*Pongamia pinnata*)	Fish oil	Microalgae	Date pit oil
Palm	*Jatropha*	Poultry fat	*Chlorellavulg*	Leather tanning waste
Safflower (Helianthus annuus)	Cotton seed *(Gossypium hirsutum)*	Pork lard	*Chlamydomonas*	
Coconut	Camelina *(Camelina Sativa)*		*Nostoc*	
Barley Peanut	*Abutilon muticum*		*Botryococcus braunii*	
Wheat	Jojoba *(Simmondsia* Chinensis*)*		*Crypthecodinium cohnii*	
Corn	*Cynara cardunculus*		*Cylindrothec*	
Sorghum	Cumaru		*Dunaliella primolecta*	
Canola	Neem *(Azadirachta indica)*		*Isochrysis*	
Rice bran (Oryza sativum)	Tobacco Seed *(Nicotiana* tabaccum*)*		*Monallanthus salina*	

Source: Adapted from Athar & Zaidi, 2020 [14].

Cheng, *et al.*, 2021 [15] shows that 13 major biodiesel-producing countries with a minimum biodiesel production of 10,000 barrels per day are the United States, Brazil, Indonesia, Germany, Argentina, France, Spain, Thailand, Poland, Singapore, Belgium, the Netherlands and Colombia. With the potential feedstocks, these countries have immense potential to increase the production of biodiesel by a large volume. For instance, countries such as Indonesia, Malaysia, Argentina, Ukraine, Canada, the Netherlands, Russian Federation, Germany, the United States, Spain, and Brazil can potentially produce 1×10^9 liters of biodiesel per annum.

Figure 1 shows potential biodiesel feedstocks in different countries.

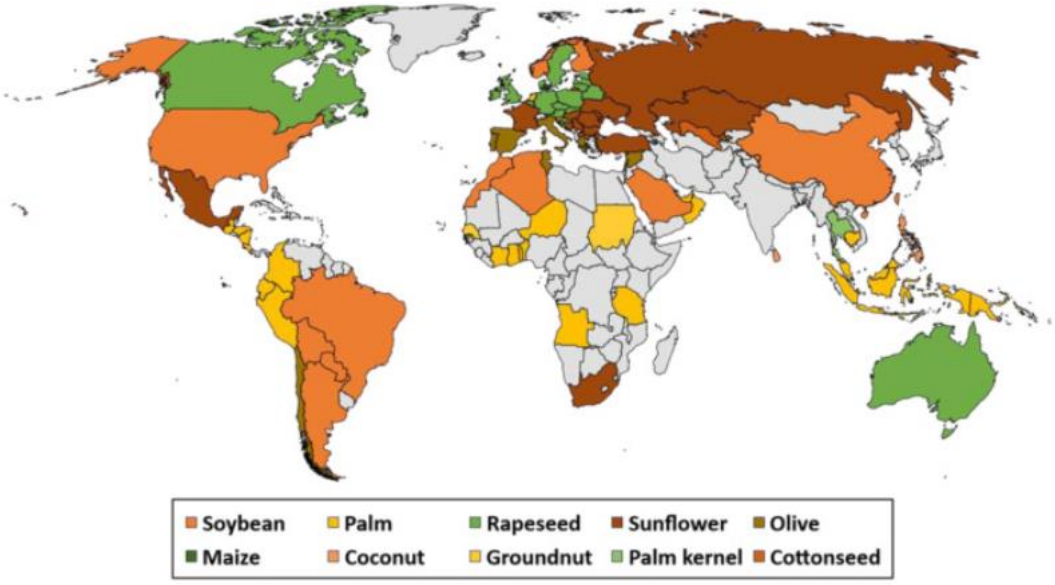

Figure 1. Potential dominant first-generation biodiesel feedstock of each country

Source: Cheng *et al.*, 2021 [15].

2.4 METHODS OF PRODUCTION

The most common methods for biodiesel production are esterification and transesterification. In both methods, it is necessary to use a fatty acid or triglyceride and an alcohol in the presence of a catalyst (basic or acid) to obtain monoesters [16].

2.4.1 Esterification

Esterification is a chemical reaction by which a FFA molecule interacts with an alcohol to produce a methyl ester plus a molecule of water. That is, the carbonyl in the carboxylic acid is initially protonated with an acid catalyst. With a more positive charge

of carbonyl carbon, the nucleophilic reaction of alcohol is more easily conducted with generation of intermediates. Then, the proton is transferred with the removal of H_2O, after that, the proton is finally eliminated with the formation of the ester [17]. The following chemical equation (see Figure 2) represents the general reaction for all industrial esterification reactions with methanol. Practically, higher amount of alcohol is introduced because esterification is a reversible reaction and requires enough alcohol in order to complete both forward and converse reactions [18].

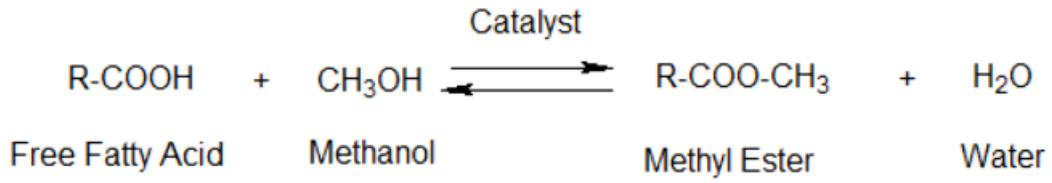

Figure 2. General Esterification mechanism.
Source: Adapted from Soltani *et al.*, 2016 [18].

2.4.2 Transesterification

Transesterification has gained much acceptance in recent years to convert vegetable oils into products with more technically compatible fuel properties. Transesterification is an imperative process to produce biodiesel since it can reduce the viscosity of the raw material / vegetable oils to a level closer to that of conventional fossil diesel. It represents an important group of organic reactions during which the exchange of the alkoxy portion results in the transformation of one ester into another. The equilibrium reaction that describes the alcoholization of carboxylic esters generally carried out in the presence of conventional catalyst (for example, NaOH and KOH) for valuable acceleration of the balance adjustment to achieve higher ester yields. Chemically vegetable oils are triglyceride molecules with structural differences in their alkyl portion linked to glycerol [14, 13].

Transesterification is the most used technique to produce biodiesel, which occurs in three stages. In the first stage, the triglyceride reacts with alcohol, generating monomolecular and diglyceride Fatty Acid Alkyl Esters (FAAE). The diglyceride then reacts

with alcohol resulting in monomolecular and monoglyceride FAAE. Finally, the monoglyceride reacts with alcohols producing monomolecular FAAE and glycerol. The transesterification mechanism is different, depending on various types of catalyst [17]. Each triglyceride molecule is made up of three long-chain fatty acid molecules of 8–24 carbon atoms connected to a glycerol backbone. Biodiesel is made up of fatty acid chains, which are chemically attached to one methanol molecule. The molecule of glycerol is almost completely removed from the final product of biodiesel. The glycerol produced as a by-product has many industrial and chemical uses. As soon as fatty acid chains break off from the triglyceride, they are known as free fatty acids (FFA). Free fatty acids are also one of the desirable biodiesel feedstocks but need different conversion processes as compared to triglycerides [14]. Figure 3 represents the general reaction for transesterification reactions with methanol.

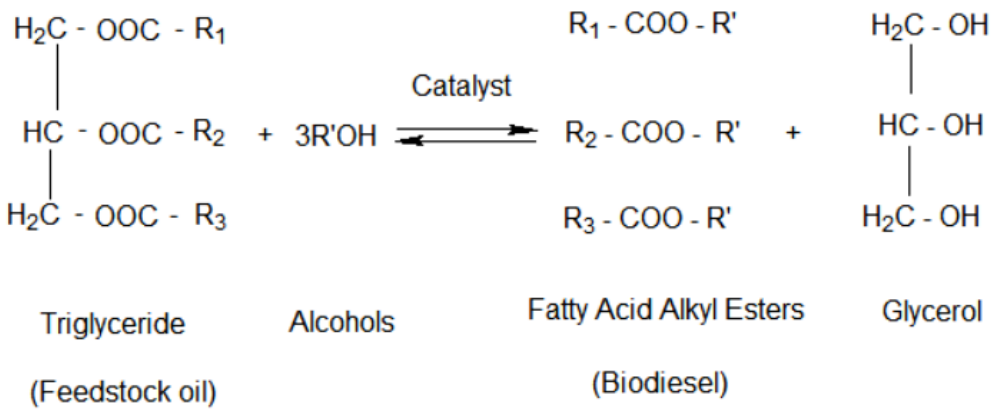

Figure 3. Transesterification mechanism.
Source: Adapted from Ma *et al.*, 2021 [17].

Various techniques of analysis have been developed to evaluate the transesterification reaction. Chromatography techniques are usually used because they offer comprehensive perception during transesterification process and detailed information required for quality control of the product. However, recently Nuclear Magnetic Resonance (NMR) spectroscopy and Fourier Transform Infrared (FTIR) spectrometry have been employed for monitoring transesterification [9].

FTIR spectroscopy is considered a powerful technique that can be used to determine the chemical structure and composition of various materials, including biological samples. Although the FTIR method is less sensitive than Gas Chromatography (GC) for quantifying minor components, by correlation with existing GC or other analytical data,

biodiesel fuel quality can be assessed through the FTIR method. Analyzing the spectra corresponding to biodiesel, the feedstock oil, and samples at intermediate conversion a method to control transesterification can be established [9].

2.5 CATALYSTS

Catalysts are used in the process of biodiesel production to increase reaction rate and efficiency of methyl ester production [2]. According to the natural property, catalysts are divided into three categories: alkaline, acid, and enzymatic. On this basis, alkaline and acid catalyst could be further subdivided into homogeneous and heterogeneous catalyst [17]. For example, NaOH, KOH, and CH_3ONa are the typical homogeneous alkaline catalysts. H_2SO_4, HCl, H_3PO_4 are the represents of homogeneous acid catalysts. Homogeneous alkaline catalysts are preferred to biodiesel production on account of fast reaction rate within short reaction time, however, such catalyst is particularly sensitive to fatty acid and H_2O in the feedstock oil, where the hydrolysis and saponification might be induced. That is to say, the feedstock oil quality ought to fulfill the strict requirement. In comparison, homogeneous acid catalysts are insensitive to FFA and H_2O, more than that, acid catalysts can catalyze the esterification of FFA. Yet, homogeneous acid catalysts are corrosive to metal facility. Nonetheless, both homogeneous alkaline and acid catalysts cannot be reused. The downstream purification is needed resulting in large number of wastewaters. To address these above problems, heterogeneous catalysts attract much interest in past decades, because they can be easily separated and reused, reducing production costs [2, 17].

The choice of solid catalyst for biodiesel production via transesterification depends on free fatty acid content in the feedstock, hence heterogeneous catalyst could provide high product yield and tolerate moisture content. These parameters are subject to quantity and strength of acidic or basic sites [10]. The transesterification process can be done with acid or basic catalysts. However, acid catalysts are not very applicable for commercial purposes, as they have some disadvantages, such as corrosion of the equipment used and a slower reaction rate. Basic catalysts are efficient than the acid catalyst in the transesterification process since the catalysis rate is 4000 times better than the acid catalyzed reaction. Although basic catalysts are inexpensive and widely available, they have certain limitations that they will work efficiently with free fatty acids at a concen-

tration of 0.5% or less. The catalyst used in the transesterification process can be classified as homogeneous acid / base catalysts, heterogeneous acid / base catalysts, and enzyme catalysts. Generally, homogeneous catalytic reactions are fast and require less concentration of catalyst when compared to heterogeneous catalytic reactions. But homogeneous catalysts are difficult to separate from the reaction mixture and reuse. In addition, it generates more residual compounds and consumes more water to remove the product from the catalyst. Heterogeneous catalysts have more advantage, as they can be recovered after the reaction, as the reaction system and heterogeneous catalysts are diphasic and require fewer washing steps to recover the catalyst. The only disadvantage in the use of heterogeneous catalyst is the reduction of activity by leaching and, therefore, the recovery of the active heterogeneous catalyst for reuse is a challenging effort. The selection or development of an active and highly specific heterogeneous catalyst is the current focus among researchers to produce high-yield biodiesel. The development of nano catalysts can solve the disadvantages of different types of catalyst, since it has a large surface area and greater catalytic property [12]. Different types of catalysts used in the production of biodiesel with their advantages and disadvantages listed in Table 3.

Table 3. Types of catalysts employed in biodiesel production.

Type of Catalyst	Examples	Advantages	Disadvantages
Acid Catalyst – Homogeneous	Sulfuric acid Hydrochloric acid and sulfonic acid	Better catalysis	Corrosion of equipment and slower rate of reaction
Acid Catalysts – Heterogeneous	Bronsted type acid catalyst, Lewis type acid catalyst, Keggin-type heteropoly-acids	The catalyst can be reusable and easy to separate	Reaction is severe and expensive to prepare catalyst
Base Catalyst – Homogeneous	Sodium hydroxide, potassium hydroxide, sodium methylate	High rate of catalysis, noncorrosive,cheap and wide availability	Soap formation at high FFA and cannot be reuse
Base Catalyst – Heterogeneous	Alkaline metal carbonates, alkaline earth metal carbonates, alkaline earth metal oxides	Catalyst can be reused, Minimal generation of waste, easier purification of product	Expensive and leaching of active sites during recovery
Enzyme Catalysts	Lipases	Highly purified product, easy to separate and reaction is mild	Methanol may deactivate the enzyme activity, high cost of operation

Source: Adapted from Manojkumar and Chandrasekaran, (2020) [12].

High acid density is an important advantage of solid acid catalyst that eases the adsorption of reactants and finally enhances the catalyst activity. Until now, a significant number of solid acid catalysts (such as sulfonic ions, sulfonated carbon based and zirconium oxide) have been used to catalyze esterification of FFAs. Generally, poor textural properties such as small surface area and low porosity, are the main concern for heterogeneous esterification catalysis. Besides, the poor textural properties limit the accessibility of the reactant particles to most active sites because there is a very low contact between the catalyst active sites and the reactant, resulting in a prolonged reaction time. Hence, the textural characteristic of the catalysts should be improved to enhance mass transfer through the porous system. A mesoporous catalysis is an innovative method which is appropriate for biodiesel preparation in both of practical and economic parts [18].

Homogeneous catalysts are used mainly despite their serious disadvantages, such as corrosive nature, difficult removal of the reaction mixture after the reaction and generation of large amounts of residual water. Acid-catalyzed reactions are generally slower than base-catalyzed reactions and require a large excess of alcohol and high pressure. When basic catalysts are used, oily or fatty raw materials must have a low content of free fatty acids (FFAs), as there is a risk of saponification of fatty acids. Heterogeneous catalysts can be easily separated from the final product, but the low reaction rate and deactivation of the catalyst are problematic. A more ecological alternative to chemical transesterification is enzyme-catalyzed transesterification, as it requires mild reaction conditions, requires less energy, reduces waste treatment, and allows a small amount of water to be present in the substrates. In addition, the ability to reuse lipases and the possibility to choose several enzymes for different substrates make this process acceptable. The high cost and inactivation of lipase by methanol, as well as impurities in crude and residual oils, represent disadvantages of this type of transesterification.

To overcome the disadvantages of existing biodiesel production processes, new technologies are emerging. The use of ionic liquids (ILs) as a catalyst, co-solvent or extraction solvent has recently attracted attention in the production of biodiesel [19].

2.6 PHYSICO-CHEMICAL CHARACTERIZATION

The standard parameters used for biodiesel characterization are specific gravity, kinematic viscosity, density, cetane number, heating value, pour point, cloud point, flash point, fire point, acid number, moisture content, saponification value, free fatty acid (FFA), ester value, peroxide value, refractive index, odor, and color. Most of these properties determine the efficiency of fuel for diesel engines [6, 20].

The density and viscosity properties are important for any liquid fuel, as they influence the performance of the injection system (pumps and injectors). In particular, at lower temperatures, where an increase in viscosity affects the fluidity of the fuel, the viscosity of the fuel becomes a problem, and it is a common practice that the maximum viscosity should not exceed a certain design limit specified by the engine manufacturer. In spray combustion on diesel compression engines, the injection system must provide the exact amount of fuel precisely adjusted to ensure efficient combustion. In this sense, density and viscosity play an important role in the spray characteristics, which are at the

heart of effective combustion processes that determine both the energy released and the emission [20].

Biodiesel usually has a high flash point (150 °C or higher). Biodiesel with a carbon chain length of less than 12 is liable for a lower flashpoint as compared to C16 and C18 chain length, which dominate in biodiesel. Oxidation stability is one more important property of biodiesel, which depends on polyunsaturated compounds of oil. Methyl ester of vegetable oils such as those of palm oil and olive oil, which are rich in saturated fatty acids, generally show improved oxidation stability. The viscosity of biodiesel is lower than that of the vegetable oils. It increases with carbon atoms present in chain length and the alcohol moiety. Viscosity also increases with the degree of saturation. A configuration like cis double-bond gives a lower viscosity than the trans double bond [14].

Cetane number (CN) is considered a qualitative measure of the ignitability of a fuel and clarifies an important aspect of the composition of, or, on a more fundamental level, the molecular structure of the compounds comprising hydrocarbon fuels in general. The scale indicates that long-chain; unbranched, saturated hydrocarbons (alkanes) have high CNs and good ignition quality while branched hydrocarbons (and other materials such as aromatics) have low CNs and poor ignition quality. The CN of D100 is currently regulated by the American Society for Testing and Materials (ASTM) commonly known by ASTM International. The society designed the ASTM D613 as a method and standard for measuring cetane number for Diesel [6, 20].

It is a common belief that higher cetane numbers provide easier starting, and quieter operation by shortening of the ignition delay period which in effect decreases the amount of fuel that is prepared to burn, thus leading to a lower rate of pressure rise and less engine noise. Theoretically, in case of too high CN, combustion can occur before the fuel and air are properly mixed, resulting in incomplete combustion and smoke. On the other hand, too low CN leads to engine roughness, misfiring, higher air temperatures, slower engine warm-up and incomplete combustion occur [20].

Water is part of any fuel at the permitted level and comes because of the processing steps. Particularly for biodiesel, the water washing process and inadequate drying techniques during manufacture or contact with excessive water during transport or storage lead to excessive water formation and can cause the fuel to be out of specification for the fuel content. In addition, excess water can lead to corrosion and provide an environment

for microorganisms, in addition to providing a cooling effect during combustion. The European standard EN 14214 therefore imposes a maximum content of 0.05 wt.% of water in fuels [20].

Table 4 summarizes the fatty acid profile of different feedstocks.

Table 4. Fatty acid profile of different feedstocks.

Fatty Acid Composition	Feedstocks							
	WCO	Coconut	Corn	Soybean	Peanut	Oil Palm	Castor	Olive Oil
Oil content (%)	-	63-65	48	15-20	45-55	30-60	53	45-70
Oil yield	-	2689	172	446	1059	5950	1413	1212
Myristic C14:0	0.41	-	-	0.09	-	-	-	-
Palmitic C16:0	0.822	7.8	6.0	10.54	11.4	45	1	9.2
Palmitoleic C16:1	0.89	0.1	-	0.27	-	-	-	0.8
Stearic C18:0	5.61	3	2.0	3.75	2.4	5	1	3.4
Oleic C18:1	48.83	4.4	44.0	23.18	48.3	40	3	80.4
Linoleic C18:2	10.94	0.8	48.0	48.92	32	10	4.2	4.5
Linoleic C18:3	2.68	0	-	2.63	0.9	-	0.3	0.6
Arachidic C20:0	0.56	-	-	0.63	-	-	-	-
Others	20.89	65.7	-	7.91	0.2		0.7	1.1

Source: Adapted from Athar and Zaidi, (2020) [21]

3. IONIC LIQUIDS

Ionic liquids are low-melting organic salts that are liquid at room temperature. They are non-volatile, thermally stable and their solvation properties vary with changes in the cation and anion. The high cost, low biodegradability, biocompatibility, and sustainability are the disadvantages of ionic liquids [1, 22].

They represent the most important class of green solvents and have attracted much interest over the past three decades in chemical community owing to their unique physical and chemical properties. The combinations of available ions and the task-specific molecular design ability make them suitable for a huge variety of tasks. But many ILs however, are hazardous and have their impact on environment. Thus, the development of alternative ILs from components that are inexpensive, non-toxic towards the environment and which are biodegradable, is the need of the hour to over-come these drawbacks. The properties of the ILs such as density, melting point, viscosity, thermal stability and solubility in water or solvents can be fine-tuned by changing either the anion or the cation [4].

The coupling of ILs with co-catalyst, such as metal ions, complexes, clusters of ligands, could further facilitate their catalytic activity of reaction process. Hence, ILs have a multitude of advantages compared to other catalysts (e.g., metal salt, zeolites, enzyme, and solid acid catalysts). Essential elements of using IL catalytic system, for instance, techno-economic and environmental aspects, can be easily addressed as they can be easily applied to a continuous process with minimal wastewater production. From an industrial standpoint, a suitable catalyst should have high reactivity and selectivity with ease of separation and reusability highly desired [1].

A new generation of ILs, called deep eutectic ILs or deep eutectic solvents (DESs), became a target of interest for many researchers studying biodiesel production due to their advantages and environmentally friendly nature. In fact, some researchers show ambivalence on whether DESs could formally be classified as ILs since they have a molecular component. Because of their complex synthesis and expensive starting reactants, ILs are more and more replaced with DESs that are formed from the mixture of organic halide salts with a complexing organic agent (usually a H-bond donor). By mixing these two components in proper ratios, eutectic mixtures are formed, which are in liquid state at temperatures below 100 °C. The complexing agent interacts with the anion and

increases its effective size, which results in decreasing the interaction between anion and cation. As a result, freezing point depression of the mixture occurs [19].

The application of ILs in biodiesel production as catalysts is increasing in recent years at least for two advantages: the possibility of their recovery and the reduced risk of contaminating the final products with them [19].

3.1 IONIC LIQUIDS IN BIODIESEL PRODUCTION

The utilization of IL in biodiesel synthesis has proven to be a good choice as it eliminates the limitations of traditional homogeneous catalysts such as difficulty in recovery and corrosiveness, as well the limitations of heterogeneous catalysts such as instability and leaching of acidity groups during reaction. Since IL acts as dual solvent-catalysts, it forms a biphasic solution upon completion of the reaction. This two-layered solution is created with the organic phase (upper layer), separated from the aqueous phase (bottom layer). This allows for biodiesel to be separated the ILs residues and substrate retaining at the lower layer. Meanwhile, it also favors the forward shift of the reaction. In addition, the extraction processes, which include liquid–liquid extraction, solid–liquid extraction, solid-phase extraction, and induced-precipitation techniques, are also favored when using IL. The use of ILs could exhibit higher biodiesel extraction yields and simple purification in comparison to those of conventional solvents and materials, as reported in a review on ILs-mediated extraction and separation processes for organic products. In this regard, the development of ILs is the most recent breakthrough as the potential alternative innovation, which has begun to yield some industrial potential in recent years [1].

3.2 LITERATURE REVIEW

Gholami *et al., (*2019) [4]investigated an alternative process, in which biodiesel was produced through transesterification of inedible Norouzak (*Salvia leriifolia*) oil in the presence of choline hydroxide (ChOH) as an ionic liquid catalyst in a microchannel reactor. An efficiency of 96.7% was obtained by the experiments for a catalyst concentration of 6.1wt.%, methanol-to-oil volume ratio of 8.8:1, temperature of 60ºC and reaction time of 12.48 min.

Phromphithak *et al.,* (2020) [23] investigated the production of methyl esters from palm oil transesterification in a microwave heated continuous flow system using choline hydroxide as a catalyst. The optimum condition was identified at molar ratio between oil to methanol of 1:12, flow rate of 20 mL/min, microwave power of 800 W and catalyst loading of 6 wt.%, temperature 68ºC and reaction time of 5 min, giving the methyl esters content 89.7%. The resulting methyl ester content was considerably lower than that obtained with the fresh catalyst. After the first reuse, the ChOH catalyst was able to generate a methyl ester content of 84.6%. The methyl ester content after fifth reuse of 49.3% occurred.

Yusuff *et al.,*(2021) [10] developed a new solid ecological catalyst from the modification of zinc anthill for methanolysis of low-grade raw material (residual cooking oil, WCO) to make biodiesel. The zinc-modified anthill was prepared by the sol-gel technique and characterized by Energy Dispersive X-Ray (EDX), Thermo Gravimetric Analyzer (TGA) / Differential Thermal Analyzer (DTA), Fourier Transform Infrared Spectroscopy (FTIR), X-Ray Diffraction (XRD), Scanning Electron Microscopy (SEM), Brunauer-Emmett-Teller (BET) and Temperature- Programmed Desorption of Carbon Dioxide (CO_2-TPD). The optimum experimental conditions obtained by a central composite design were 17.99:1 for the molar ratio of methanol to WCO, 0.51 wt.% of catalyst loading (ZnMA), temperature of 66.54 °C and reaction of 2 hours. According to gas chromatography analysis, the fatty acid methyl ester conversion under optimum conditions was 97.05%. Based on the FAME yield obtained, zinc oxide supported anthill is assumed as suitable heterogeneous catalyst for renewable fuel production and thus should be tested with various oil types.

Sahar *et al.,* (2018) [24] studied transesterification reaction of waste cooking oil (WCO) in the presence of alkali catalyst (KOH). The acid value of WCO was 5.5 mg

KOH/g which indicated high FFA content. The optimum conditions were 1:2.5 methanol to oil molar ratio, 1 wt.% of catalyst, with a temperature of 50ºC for 1 hour, and Fatty acid methyl ester (FAME) yield was 94%.

Rosset and Perez-Lopez, (2019) [9] evaluated double layer hydroxides, mixed oxides and pure oxides based on magnesium and calcium as catalysts in the methyl transesterification of soybean oil in a batch reactor. The catalysts were prepared by continuous coprecipitation and characterized by specific surface area, thermogravimetric analysis, CO_2 desorption programmed by temperature and X-ray diffraction. The reactions were carried out at 65 ° C, methanol/soybean oil molar ratio of 9:1, catalyst dosage of 1wt.% by weight and reaction time of 240 min. achieving a conversion yield of 90%.

Adeyinka *et al.,* (2021) [25] characterized and developed the fly ash compound of zinc carbon-oxide (CFA/ZnO) as a catalyst in the transesterification of used cooking oil (UCO) with methanol. The optimal experimental conditions were temperature of 140 ° C, time of 3 h, methanol / molecular oil ratio of 12: 1 and catalyst load of 0.5% by weight, the biodiesel yield was 83.17%. The FAME content of the biodiesel produced was 98.14% by weight. In addition, the regeneration and reuse of the catalyst was studied to verify its stability, and it was established that CFA-ZnO could be reused for up to four successive cycles with negligible loss of performance.

Fan *et al.*, (2013) [26] explored the catalytic synthesis of biodiesel from soybean oil by transesterification over basic ionic liquid catalysts, choline hydroxide (ChOH), choline methoxide (ChOMe) and choline imidazolium (ChIm) at atmospheric pressure. Among the selected ionic liquids, ChOH exhibited the best catalytic performance. The biodiesel yield reached 95.0% when the molar ratio of methanol and soybean oil was 9:1, the optimum catalyst dosage 4 wt.%, at 60 °C for 2.5 hours.

Table 5 summarizes the information discussed above about some experimental conditions found in the literature to produce production biodiesel.

Table 5. Some experimental conditions found in the literature for biodiesel production.

Reaction Type	Trans.	Trans.	Trans.	Trans.	Trans.	Trans.	Trans.
Feedstock	Norouzak oil	Palm oil	WCO	WCO	Soybean oil	UCO	Soybean oil
Catalyst	[ChOH]	[ChOH]	[ZnMA]	[KOH]	[CaO]	[ZnO]	[BMIM] OH
Molar Ratio Alcohol: Oil	1:8.8	1:12	17.99:1	1:2.5	9:1	12:1	9:1
Catalyst Dos-age(wt%) (wt%)	6.10	6.00	0.51	1.00	1.00	0.50	4.00
Temperature (ºC)	60.00	68.00	66.54	50.00	65.00	140.00	60.00
Reaction Time (min)	12.48	5	120	60	240	180	150
FAME con-tent (%)	96.70	89.70	97.05	94.00	90.00	98.14	95.00
REF	[4]	[23]	[10]	[24]	[9]	[25]	[26]

3.3 CHOLINE HYDROXIDE

Choline hydroxide (ChOH) is a non-toxic and naturally abundant task-specific that can be used to carry the hydroxide ion into organic systems (Figure 4). It is water-soluble and can be easily prepared from biodegradable and low-cost starting materials in high purity. Moreover, it is an excellent phase transfer catalyst in terms of activity and selectivity [27]. It is considered an environment-friendly catalyst due to the presence of choline cation. Moreover, this substance can be recovered and reused in the transesterification process. Due to its inexpensive raw materials and their availability, choline hydroxide is considerably less expensive compared to other ionic liquids [4].

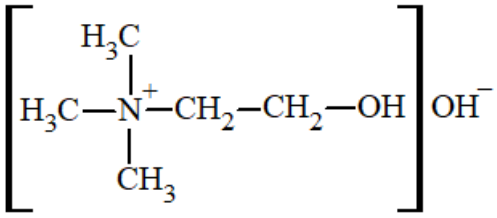

Figure 4. Structure of choline hydroxide.

Source: Fan *et al.*, (2013) [26].

Choline hydroxide is a strong organic base with application in the production of other choline salts and in processes where a strong base with low levels of inorganic ions is necessary or tolerated. The industrial production of choline hydroxide includes reacting at a temperature above 30 ° C, ethylene oxide, trimethylamine, and water in the presence of an aqueous medium in quantities such that they form a diluted solution of choline hydroxide having a concentration below 40%. This diluted solution is concentrated by removing water to give a choline hydroxide solution at least 1.05 times more concentrated than the initial solution [28].

Choline is an essential nutrient that supports important functions in the body, such as that involved in the synthesis of phosphatidylcholine, in the formation of acetylcholine and in the metabolism of a carbon. Like choline hydroxide, choline hydroxide, commonly referred to as 2-hydroxy-N, N, N-trimethyl-1-ethanaminium hydroxide, is widely used as an intermediate for organic synthesis in biochemical research. Choline hydroxide plays a key role in promoting the generation of hydrogen in fuel cells, using as a structure-directing agent, and in the preparation of catalysts. Therefore, the production of high-purity choline hydroxide presents a great prospect in the industry [29].

Common methods for the preparation of choline hydroxide are chemical synthesis, electro-electrodialysis (EED) and ion exchange absorption. Usually, the chemical synthesis method consists of the direct reaction of triethylamine with water and ethylene oxide to obtain choline hydroxide by the phase separation process. Unfortunately, the choline hydroxide produced has a strong basicity, so this method is prone to generate by-products like monoethoxycholine, diethoxy choline and ethylene glycol. The other two approaches to synthesizing choline hydroxide are carried out using the choline chloride (CC) reaction. The EED method integrates the selective transport of anionic / cation exchange membranes and the division of water formed at the cathode and anode, dissociates the CC in choline hydroxide and hydrochloric acid. In this process, the chlorine gas generated can occur a series of reactions with the solution that leads to the formation of the multicomponent product. Ion exchange absorption is based on the purpose of exchanging the Cl− into OH− by passing the CC solution through the strongly basic anion exchange resin treated with OH−, to obtain the desired choline hydroxide solution. Although pure choline hydroxide can be obtained, a considerable amount of waste acidic and basic solutions will be generated during the process of cleaning and regenerating the ion exchange resin [29].

In summary, the traditional production methods of choline hydroxide have several disadvantages, which are the low yield, low purity of the products, the high consumption of energy or other reagents and seriously environmental pollution [29].

3.3.1 CHOLINE HYDROXYDE SYNTHESIS

Choline hydroxide (ChOH) is synthesized by the reaction between equimolar choline chloride and potassium hydroxide in methanol, as shown in Figure 5. The solution is subjected to reflux at 60 °C for 24 h. Thereafter, it is cooled to ambient temperature and potassium chloride (KCl) is separated by filtration. The excess methanol is removed from the mixture by evaporation to attain the ChOH catalyst [16, 30].

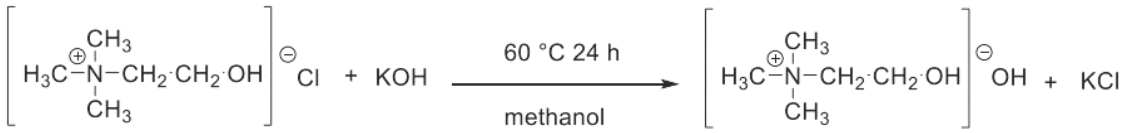

Figure 5. Synthesis of choline hydroxide using choline chloride and potassium hydroxide.

Source: Phromphithak *et al.*,2020 [23]

3.4 REVIEW OF PREVIOUS WORKS

The following is a brief outline off all the works done so far by the research group with a focus on the production of biodiesel using ionic liquid as catalysts.

R. Lima (2020) [16] synthesized the catalyst choline hydroxide (ChOH) and compared it with a commercial catalyst solution, which resulted in a correlation of approximately 85%. Nevertheless, the commercial choline hydroxide was selected to be applied in the biodiesel production from residual and virgin sunflower oil. The best conversion values were obtained under the following conditions: 4% of catalyst, molar ratio oil/methanol of 1:8, and 1 hour of reaction, for a temperature settled at 65 °C for all the reactions.

A. Lima (2020) [31] studied the application of alkaline type ionic liquids in the catalysis of transesterification reactions of mixtures of triacylglycerols. The reaction with choline hydroxide presented 85.21% of conversion in FAME content in 30 minutes, with 2wt.% of catalyst, 1:10 oil/methanol molar ratio at 65ºC. A kinetic study was carried out demonstrating that a second-order model was the best fit for the reaction with a rate constant (k) estimated as 0.2930 $L.mol^{-1}.min^{-1}$. From the recovery of the IL, it was possible to conclude that although there was some separation of it from the glycerol by the extraction with butanol and water, an amount of ChOH remained in glycerol phase.

Belhaj (2019) [32] studied the performance of [HMIM][HSO_4] catalyst using different amounts of the IL (10%, 15%, and 20%) in the esterification of oleic acid and methanol, for the conditions of 1:10 oil/MeOH molar ratio, a reaction time of 4 hours, and reaction temperature of 65 °C. Among the reactions for each amount of catalyst, the highest conversion was found for the catalyst dosage of 15%. Two methods for drying the aqueous samples (lower phase of biodiesel production through esterification) were applied for the recovery of the IL. The first one implied the drying of the sample in an oven at 110°C, and the other one was a drying process in a vacuum oven at 60°C/70 °C. From the application of the recovered IL in new reaction cycles, the highest conversions were obtained with an amount of catalyst of 20%, which after 4 cycles was 59.39%.

Meireles (2018) [33] aimed to evaluate [BMIM][$MeSO_4$] IL as a catalyst for the esterification process of oleic acid with methanol. The study showed the highest conversion of 92.4% for the following operational conditions: 10 wt.% of catalyst load, molar ratio of 1:10 OA/MeOH, a reaction time of 8 hours, at 65 °C. To determine the order of the esterification reaction, a study was carried out using 10% wt. of catalyst, OA/MeOH

molar ratio of 1:6 for 4 hours, for the temperatures of 45.50 and 65 °C. The parameters for the kinetic study were estimated as 57.9 kJ/mol for the activation energy, and a pre-exponential factor of 0.0448 $L.mol^{-1}.min^{-1}$. The recovery of the ionic liquid was tested using three different methods: drying, rotary evaporator, and washing with different solvents. The application of the various processes in the recovery of the IL showed a very low correlation, which shows that the recovered IL contains unknown impurities. The purity of the recovered IL was verified through FTIR analysis, for the samples of IL at 20% (w /w), demonstrating a correlation of 96%. Thus, because it is an acid-catalyzed esterification, and the IL is hydrophilic, the best recovery method performed was using water in the washing process.

Roman (2018) [34] studied the behavior of the catalyst [HMIM][HSO_4] through the esterification reaction of oleic acid. The optimum conditions for the conversion were determined as 8 h, 110 °C, OA/MeOH molar ratio of 1:15 and a catalyst dosage of 15 wt.%, resulting in a conversion of 95%, and for the FAME content were 8 h, 110 °C, OA/MeOH molar ratio of 1:14 and a catalysts dosage of 13.5 wt.%, leading to a content of 90%. The kinetic experiment was carried out using the best conditions for the conversion for a temperature range varied from 70 °C to 110 °C. The results were well described using a third-order reaction model, and it was found an activation energy of 6.8 kJ/mol and a pre-exponential factor of 0.0765 $L^2.mol^{-2}.min^{-1}$.

Tadevosyan (2017) [35] analyzed the influence of several ionic liquids as catalysts in the esterification reaction of OA. Among five ILs, [BMIM][HSO_4], [BMIM][CH_3SO_3], [BMIM][CH_3SO_4], [MIM][HSO_4], and tributylmethylammonium methyl sulfate. The values obtained for the conversion for the esterification reaction showed that the ionic liquid [BMIM][HSO_4] was the most promising one. From this result, the recovery of the IL was studied, and several esterification reactions of oleic acid were carried out using a catalyst dosage of 10 wt.%, 15 wt.%, and 20 wt.% relative to the mass of OA. The parameters used for the reactions were: reaction temperature of 90 °C, a reaction time of 6 hours, and an oil/MeOH molar ratio of 1:10. It was verified that with the increase of catalyst dosage, there was an increase in the FAME content so that, the best amount of catalyst applied to the system was 20% with 84.8% of conversion. In the first reaction, a conversion of 84.90% was obtained, and by the fifth cycle, it was obtained 77.10%.

Alimova (2016) [36] evaluated the behavior of different operating parameters in the esterification of oleic acid with methanol into biodiesel with an acidic IL,

[BMIM][HSO_4]. Reactions were carried out with various amount of ionic liquid (2.5wt.%; 5wt.%; 7.5wt.%; 10wt.%; 12.5wt.%) with constant temperature and reaction time. The yield of the product went from 85.0% to 89.7% when the percentage of catalyst increased from 2.5wt.% to 10wt.%, but then there was a sharp drop. At 90 ºC the biodiesel yield reached 53.4% of reaction conversion. The optimum conditions for the esterification were identified as an OA/MeOH molar ratio of 1:10, a catalyst amount of 10 wt.%, a reaction time of 4 h, and a reaction temperature of 90 ℃.

Diniz (2020) [37] aimed to evaluate [HMIM][HSO_4] IL as a catalyst for esterification/transesterification reactions in WCO samples and to study the maximum number of recovery cycles that can be performed with IL without significant yield of loss reaction. Oleic acid (OA) and a simulated oil with a high acid content, prepared by mixing 40% OA and 60% by weight of WCO, were used as raw materials. The reaction conditions selected were a temperature of 65 ° C, a reaction time of 4 hours, a molar ratio of 1:10 of raw material/methanol and 10% of catalyst. Using OA as raw material, an initial conversion of 81.2% was obtained, in terms of drop in acidity. After seven reaction cycles, the conversion dropped to 69.4%, while the content of fatty acid methyl esters (FAMEs) in the biodiesel produced decreased from 64.7% to 57.5%. When using simulated oil as a raw material, an initial conversion of 45.6% was obtained and after nine reaction cycles the conversion dropped to 27.2%, while the FAME content of biodiesel decreased from 24.1% to 14. 0%. The correlation between FTIR spectra relating IL after the last reaction cycle and the initial IL was 99.3% for reactions using OA and 90.0% when using simulated oil, showing that the water wash recovery method is efficient.

A summary of what was exposed above is presented in Table 6.

Table 6. Summary of preview works done by the research group.

Work	R. Lima (2020)	A.Lima (2020)	Diniz (2020)	Belhaj (2019)	Meireles (2018)	Roman (2018)
Reaction Type	Trans.	Trans.	Esterif./ Trans.	Esterif.	Esterif.	Esterif.
Feedstock	CO	Sunflower oil	WCO	OA	OA	OA
Ionic Liquid	[ChOH]	[ChOH]	[HMIM] [HSO_4]	[HMIM] [HSO_4]	[BMIM] [$MeSO_4$]	[HMIM] [HSO_4]
Molar Ratio Oil/Methanol	1:8	1:10	1:10	1:10	1:10	1:15
Catalyst Dosage (wt.%)	4	2	10	15	10	15
Temperature (ºC)	65	65	65	65	65	110
Reaction time (h)	1	30min	4	4	8	8
Conversion (%)	96.06	85.21	45.6	91.26	92.40	95.00
REF	[16]	[31]	[37]	[32]	[33]	[34]

4. TECHNICAL DESCRIPTION AND PROCEDURES

4.1 REAGENTS AND RAW MATERIALS

The reactants used for the transesterification reaction was choline hydroxide, purchased from Sigma Aldrich, methanol from LabChem and Carlo Erba, oleic acid (tech.90%), obtained from Alfa Aesar (Germany) and waste cooking oil, from restaurants in the region of Bragança, Portugal.

The materials utilized for characterization and analysis were n-heptane (99%), and sodium sulfate anhydrous purchased from Carlo Erba. Diethyl ether and ethanol were obtained from Honeywell. Borax was obtained by Riedel-de-Haën. Concentrated hydrochloric acid, potassium hydroxide, 37 FAME mixture, the methyl heptadecanoate (99%), and boron trifluoride-methanol solution were purchased from Sigma Aldrich. Phenolphthalein indicator (99%), and sodium chloride were obtained by Panreac.

4.2 EQUIPMENT

For biodiesel synthesis, two heating plates with automatic temperature control and magnetic stirring (IKA, model C-MAG HS4 digital and VWR, model VMS-C4), using a condenser to reflux the excess of methanol from the reaction solution was used. For phase separation of the transesterification reaction product, a centrifuge (EPPENDORF, model 5810 R) was utilized, and for drying the phases, an oven (SCIENTIFIC, series 9000). The samples masses were measured with an analytical balance with a precision of ±0.0002 g (AE, model ADA 210/C). The FAMEs content in biodiesel samples was evaluated in a gas chromatograph system chromatograph (SHIMADZU Nexis GC-2030) equipped with an FID detector, an autoinjector AOC- 20i, and an OPTIMA BioDiesel F (30mx0.25mmx0.23μm) capillary column. For infra-red spectroscopy, a PerkinElmer spectrometer, model Spectrum Two FT-IR with a Universal ATR accessory was used.

4.3 METHODOLOGY

The experimental part of this work involves carrying out various transesterification tests using choline hydroxide to produce biodiesel from waste cooking oils. For the transesterification reactions, the methodology used was the methodology already validated within the research group [16, 31, 32, 33, 34, 35, 36, 37] and cited by several authors to produce biodiesel.

4.3.1 Transesterification Reaction of waste cooking oil

The transesterification reactions were carried out in a glass reactor (two-necked flask), with a capacity of 250 mL (1) as shown in Figure 6. First, a defined mass of cooking oil, oleic acid and choline hydroxide solution are weighed on an analytical balance. Then, the reactor was immersed in a paraffin bath (2), which was coupled with a reflux condenser (3) and placed over an automatic heating plate with agitation (4) and automatic temperature control. An extra thermometer is used to confirm the temperature inside the solution (5) and when the temperature reaches the desired value in this thermometer, methanol is added, starting the reaction. Furthermore, a temperature probe (6) is placed which is used to control the temperature in the paraffin bath.

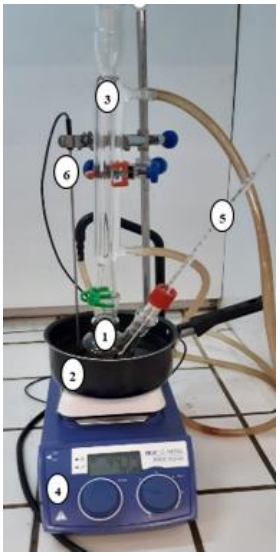

Figure 6. Experimental apparatus for the transesterification reaction to produce biodiesel.

The reaction conditions, such as catalyst percentage, WCO/methanol molar ratio, incorporation of oleic acid, temperature, vary according to the optimized parameter. In this work, a constant reaction time of 30 minutes was maintained, varying the other reaction parameters.

At the end of the reaction, stirring is stopped, the flask is removed from the bath and the resulting mixture is left to cool in cold water to stop the reaction. Then, the mixture was transferred to a separating funnel for phase separation for at least 24 hours. The two phases, the organic phase containing biodiesel and the phase with glycerol and choline hydroxide, are separated, as shown in Figure 7, their individual masses are weighed, placed in centrifuge tubes, and taken to centrifugation at 3000 rpm per 30 minutes for more efficient separation.

With the aid of a Pasteur pipette, the phases obtained by centrifugation are again separated, their masses measured and placed in identified 15 mL flasks, as shown in Figure 8. After that, the samples were dried in an oven at 110 °C for approximately 24 h, then stored in the fridge until the moment of analysis.

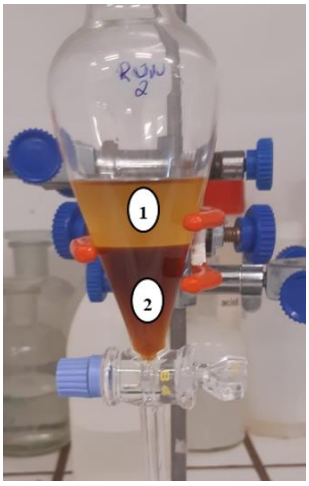

Figure 7. Phase separation; Phase (1): organic or biodiesel phase. Phase (2): glycerol + catalyst phase.

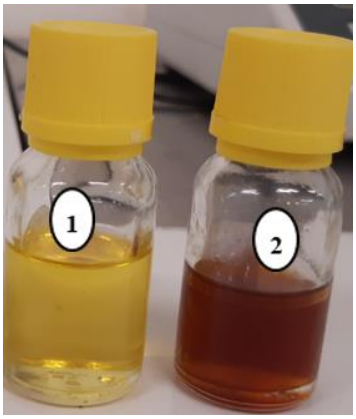

Figure 8. Phase separations in 15 mL flasks; (1): Light phase, (2): Heavy phase.

After drying, the organic phase is analysed by GC-FID, to determine the FAME content of each sample, to later calculate the reaction conversion.

4.3.2 FAME content by Gas Chromatography

The fatty acid methyl ester (FAME) content of the produced biodiesel was characterized by gas chromatography with FID detector (GC-FID) analysis in compliance with the procedures described in European Standard EN14103 [38, 39]. This analytical technique provides the distribution area corresponding to each component present in the sample. Figure 9 shows the equipment used to perform these analyses.

Figure 9. GC-FID equipment used for FAME content analysis in biodiesel samples.

The operating conditions used in every GC analysis were based on a helium flow of 1 $mL.min^{-1}$, an oven temperature program which started with a temperature of 50 °C, maintained for 1 min and followed by an increase in temperature up to 200 °C at a rate of 25 °C/min. Then, it was once again increased to 230 °C with a heating rate of 3 °C/min for 3 min. The final temperature was maintained for 23 min, for a total running time of 40 min. The injector was operated at 250 °C. The injector was used in split mode, with a split ratio of 1:100, and the detector temperature was 250 °C, and the injected sample volume was 1 µL.

For GC-FID analysis, the biodiesel samples were prepared as follows: on an analytical balance, approximately 250 mg of the biodiesel sample was measured in a 10 ml bottle, using a micropipette for this purpose. Then, 5 mL of methyl heptadecanoate standard solution, used as an internal standard, with known concentration of 10 mg / mL was added. A small amount of anhydrous sodium sulfate was added to remove any remaining moisture in the samples. Then, the solution was agitated and left to stand for at least 2 min, and a sample volume of 1 mL was transferred to a 2 mL GC vial to perform the GC analysis.

The identification of each methyl ester present in the sample is performed by comparison with the retention time of the analysis of the mixture of FAME compounds obtained in this work with the GC Shimadzu system under the operational conditions mentioned above with the retention times obtained in other analyzes provided by the manufacturers. One is the chromatogram obtained from the same mixture of 37 FAME compounds supplied by Supelco using an Omegawax ™ 250 column, shown in Figure 6.

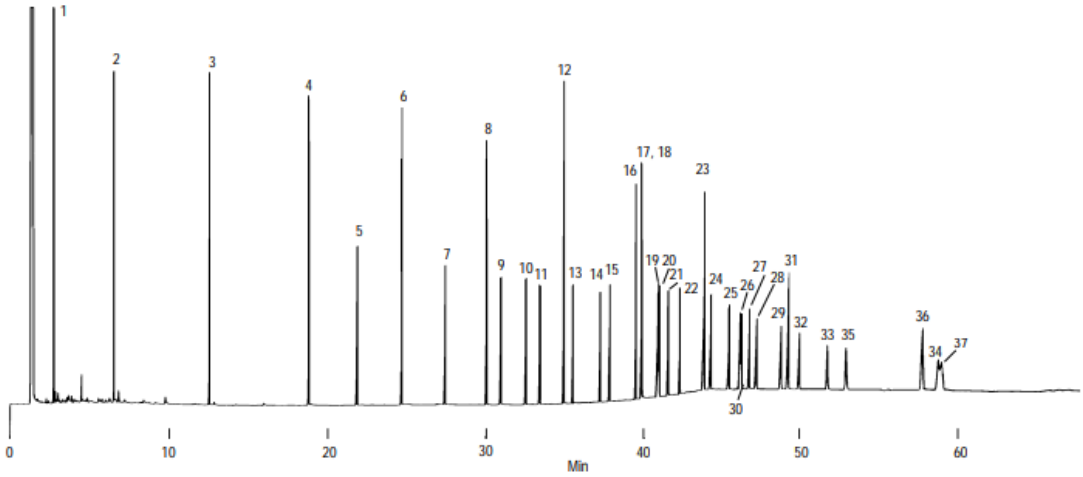

Figure 10. Chromatographic analysis obtained for the Supelco 37 Component FAME. Mix on the Omegawax 250 column.

Source: Adapted from Supelco [40].

The FAMEs present in the biodiesel samples are identified by comparing the retention time of the peaks present in the chromatogram, with the retention time of the FAMEs obtained by analyzing the standard mixture. After identifying the FAMEs present in the biodiesel sample, their content (C) is calculated by Equation (1), using the individual area of each compound, the area of methyl heptadecanoate, used as an internal standard and the sum of all areas of all compounds identified as FAMEs.

$$\%\ \mathrm{FAME} = \frac{\sum \mathrm{A_{FAMEs}} - \mathrm{A_{IS}}}{\mathrm{A_{IS}}} \times \frac{\mathrm{C_{IS}} \times \mathrm{V_{IS}}}{\mathrm{m_{biodiesel}}} \times 100 \qquad (1)$$

Where $\sum A_{FAMEs}$ is the total peak area of all methyl esters from C4:0 to C22:0; A_{IS} is the peak area corresponding to methyl heptadecanoate, used as internal standard, C_{IS} is the concentration, in milligrams per milliliter, of the methyl heptadecanoate solution, V_{IS} is the volume, in milliliters, of the methyl heptadecanoate solution, and $m_{biodiesel}$ is the mass, in milligrams, of the biodiesel sample.

Equation (1) shows the total contribution of FAME and to calculate the individual contribution of each FAME, Equation (2) is used:

$$C_n(\%) = \frac{\sum A_{FAMEs}(n)}{A_{IS}} \times \frac{C_{IS} \times V_{IS}}{m_{biodiesel}} \times 100 \quad (2)$$

Where $C_n(\%)$ is the contribution of FAME(n) in the sample, expressed as a mass fraction, and $A_{FAMEs}(n)$ is the area of compound n. For the final percentage of conversion, only compounds with percentages above 1% were considered.

Equation (3) shows the yield of the biodiesel produced.

$$\text{Yield } (\%) = \frac{m_{biodiesel} \times \%FAME}{m_{inicial\ of\ the\ WCO}} \quad (3)$$

Where $m_{biodiesel\ produced}$ is the mass of the biodiesel produced in grams, $\%FAME$ is the percentage in FAME of the biodiesel and $m_{inicial\ of\ the\ WCO}$ is the mass of the oil used in the reaction in grams.

Table 7 shows the elution order, compound name, compound ID, retention time and the obtained chromatographic area, for the analysis of the Supelco 37 compound FAME mix used. This table is used to identify each FAME peak in the analysed samples. These peaks are subsequently selected for the estimation of the individual FAME contents, and the total FAMEs content, in the biodiesel samples.

Table 7. Elution order, compound name, compound ID and retention time for the 37 compounds.

Elution Order	Peak name	Peak ID	Retention time (min)	Area (µV)
1	Butyric acid methyl ester	C4:0	3,621	30583
2	Caproic acid methyl ester	C6:0	4,953	37694
3	Caprylic acid methyl ester	C8:0	6,25	42455
4	Capric acid methyl ester	C10:0	7,416	45648
5	Undecanoic acid methyl ester	C11:0	8,007	23521
6	Lauric acid methyl ester	C12:0	8,629	48399
7	Tridecanoic acid methyl ester	C13:0	9,31	24745
8	Myristic acid methyl ester	C14:0	10,084	50129
9	Myristoleic acd methyl ester	C14:1	10,427	24033
10	Pentadecanoic acid methyl ester	C15:0	10,982	25267
11	cis-10-Pentadecanoic acid methyl ester	C15:1	11,389	25247
12	Palmitic acid methyl ester	C16:0	12,036	82633
13	Palmitoleic acid methyl ester	C16:1	12,381	28309
14	Heptadecanoic acid methyl ester	C17:0	13,263	45323
15	cis-10-Heptadecanoic acid methyl ester	C17:1	13,662	25536
16	Stearic acid methyl ester	C18:0	14,677	52918
17,18	Oleic acid methyl ester, Elaidic acid methyl ester	C18:1 (c+t)	15,033	92760
19,20	Linoleic acid methyl ester, Linolelaidic acid methyl ester	C18:2 (c+t)	15,784	59824
21	gamma-Linolenic acid methyl ester	C18:3n6	16,315	25316
22	Linolenic acid methyl ester	C18:3n3	16,891	25721
23	Arachidic acid methyl ester	C20:0	18,068	52296
24	cis-11-Eicosenoic acid methyl ester	C20:1	18,541	25933
25	cis-11,14-Eicosadienoic acid methyl ester	C20:2	19,618	25832
26,27	cis-8,11,14-Eicosatrienoic acid methyl ester, Heneicosanoic acid methyl ester	C20:3n6, C21:0	20,304	51710
28	cis-11,14,17-Eicosatrienoic acid methyl ester	C20:3n3	20,92	22562
29	Arachidonic acid methyl ester	C20:4n6	21,276	24669
30	cis-5,8,11,14,17-Eicosapentaenoic acid methyl ester, Behenic acid methyl ester	C20:5n3	22,811	24184
31	Behenic acid methyl ester	C22:0	23,08	53019
32	Erucic acid methyl ester	C22:1	23,832	25793
33	cis-13,16-Docosadienoic acid methyl ester	C22:2	25,582	24786
34	Tricosanoic acid methyl ester	C23:0	26,629	25197
35	Lignoceric acid methyl ester	C24:0	31,164	49429
36, 37	cis-4,7,10,13,16,19-Docosahexanoic acid methyl ester, Nervonic acid methyl ester	C22:6n3, C24:1	32,393	47595

4.4 VOLUMETRIC MEASUREMENTS

4.4.1 Acidity Measurement

The acid value was determined to measure the degree of occurrence of free fatty acids (FFAs) present in waste cooking oil and oleic acid used in the study, and the calculation was performed following EN 14104 Standard [92]. Initially, 1 gram of oil sample was transferred to an Erlenmeyer using a micropipette, and an analytical balance was used to measure the weight. After this, 25 mL of the solvent 1:1 (v/v) ethanol/diethyl ether and 5 drops of phenolphthalein was added into the flask. Then, the solution was titrated with a standard solution of potassium hydroxide. The acid value is given in terms of mg of KOH/g sample by Equation (4).

$$\mathrm{AV} = \frac{\mathrm{V_{KOH}} \times \mathrm{C_{KOH}} \times \mathrm{MW_{KOH}}}{\mathrm{m_{Sample}}} \quad (4)$$

In this equation, V_{KOH} is the volume, in mL of the KOH solution used in the titration, C_{KOH} is the concentration of the KOH solution, in mol.L^{-1}, MW_{KOH} is the KOH molecular weight, which is 56.1 g.mol^{-1}, and m_{Sample} is the oil masses samples measured, in g.

4.4.2 Determination of basicity of choline hydroxide solution in methanol

The determination of the concentration of hydroxyl ion present in the solution of choline hydroxide in methanol was done through an acid-base titration, using a standard solution of HCl as the titrant and methanol as the solvent. A certain mass of the solution was weighed and titrated. So that the volume of titrant used did not exceed 25 mL, the theoretical volume of HCl needed was determined using Equation (5). The percentage of choline hydroxide in the methanol solution that was used as the basis for this calculation was the percentage indicated on the label of commercial choline hydroxide, which was 45%.

$$V_{HCl} = \frac{n_{HCl}}{[HCl]} \times 1000 \quad (5)$$

Where V_{HCl} is the theoretical volume of HCl, in mL, used for a given mass of choline hydroxide solution in methanol. The n_{HCl} is equal to the number of moles of

ChOH, which is calculated by Equations (6) and (7) below, $[HCl]$ is the concentration of HCl.

$$m_{ChOH} = m_{ChOH(CH_3OH)} \times 0.45 \quad (6)$$

$$n_{ChOH} = \frac{m_{ChOH(CH_3OH)}}{MW_{ChOH}} \quad (7)$$

The $m_{ChOH(CH_3OH)}$ is the mass of the titrated methanolic choline hydroxide solution, in grams, the value of 0.45 is the theoretical percentage of choline hydroxide in the solution.

Knowing the heavy masses and spent volumes of HCl, it is possible to calculate the real percentage of ChOH in the choline hydroxide solution in methanol, by Equations (8), (9) and (10).

$$n_{ChOH(real)} = \frac{V_{HCl}}{1000} \times [HCl] \quad (8)$$

$$m_{ChOH(real)} = n_{ChOH(real)} \times MW_{ChOH} \quad (9)$$

$$\%\ ChOH\ na\ reação = \frac{m_{ChOH(real)} \times 100}{m_{ChOH(CH_3OH)}} \quad (10)$$

Thus, in Equation (4) the volume of HCl is divided by 1000 for unit adjustment. In Equation (6), the actual mass of ChOH is multiplied by 100 because 100 g of solution was used as the base.

4.5 DERIVATIZATION OF FATTY ACIDS BY BF_3

The derivatization procedure of the methyl esters of fatty acids by boron trifluoride (BF_3) was performed to determine the distribution of the fatty acids present in the feedstock used in the production of biodiesel, and decrease the potential damage to the column and/or instrument [38].This process consists of the transformation of the triacylglycerols and fatty acids present in the sample feedstock into methyl esters, followed by the quantification of compounds between Myristic acid methyl ester (C14) and Lignoceric acid methyl ester (C24) by gas chromatography.

Initially, the necessary solutions of methanolic KOH and methyl heptadecanoate were prepared. The methanolic KOH solution was prepared by adding the proper amount of potassium hydroxide in methanol to make a 0.5 $mol.L^{-1}$ solution.

Thus, 25 mg of the feedstock sample and 2.5 mL of the methanolic solution of KOH (0.5 $mol.L^{-1}$) were added to a 20 mL flask. Then, the flask was closed and submitted to a drying process in an oven at 90 °C for 10 min, thereafter, it was removed from the oven and waited to cool to room temperature. 2 mL of BF_3 in methanol solution (10%, v/v) was added in the flask, and it was closed and placed in the oven at 90 °C for more 30 min. Again, it was removed from the oven and allowed to cool to room temperature. After that, 3 mL of methyl heptadecanoate solution was added in the solution, and it was agitated using a vortex apparatus. Then, 2 mL of saturated sodium chloride solution was added, and the solution was subjected once again to the vortex agitation. The sample was centrifuged for 5 min at 3000 rpm for the separation of the two phases. By the end, 2 mL of the upper phase was reserved into a 4 mL flask. A small amount of anhydrous sodium sulfate was added to remove all moisture present before gas chromatography analysis was performed.

4.6 FTIR ANALYSIS

The FTIR (Fourier-Transform Infrared Spectroscopy) analysis offers some information required to identify the chemical components and functional groups in a compound [10]. It is an analytical technique used to identify organic materials, polymers, and some inorganic components. The FTIR analysis method uses infrared light to analyze how tests work and observe applied properties. The FTIR sends infrared radiation of about 10,000 to 100 cm^{-1} through a sample, with some radiation being absorbed and others not. The absorbed radiation is converted into rotational and / or vibrational energy by the sample molecules. The resulting signal in the detector is presented as a spectrum, detector from 400 to 4500 cm^{-1} in a resolution of 4 cm^{-1} and 4 cumulative scans, representing a molecular fingerprint, making FTIR analysis a great tool for chemical identification [31].

Figure 11 shows the equipment used in this work for the FTIR analyses.

Figure 11. Perking Elmer FTIR, Spectrum Two model.

4.7 EXPERIMENTAL DESIGN

The Box-Behnken Design (BBD), which is the standard Response Surface Methodology (RSM), was applied to evaluate the effects of transesterification reaction on acidity value, FAME content and the yield percentage of biodiesel. Table 9 shows the experimental design, four parameters was evaluated at three levels (-1,0 and 1) with 27 experimental runs and three central points. The parameters chosen as control factors were reaction temperature (55, 60 and 65ºC), oil/methanol molar ratio (1:5, 1:10 and 1:15), the percentage of catalyst (0.7, 1.4 and 2.1 wt%) and the incorporation of oleic acid (0, 1 and 2 wt%). The time was fixed at 30 minutes.

The experimental runs of the experimental conditions are presented in Table 8.

Table 8. Experimental information of independent variables in BBD

Parameters	Code	**-1**	**0**	**+1**
Temperature (ºC)	A	55	60	65
Molar ratio oil/methanol	B	1:5	1:10	1:15
Catalyst dosage (%wt)	C	0.7	1.4	2.1
Incorporation of oleic acid (%wt)	D	0.0	1.0	2.0

The methodology allows fitting a quadratic mathematical model that describes the relationship between the parameters and each response. The generic formula for the mathematical model is given by Equation (11).

$$Y = \beta_0 + \sum_{i=1}^{k} \beta_i X_i + \sum_{i=1}^{k} \beta_{ii} X_i^2 + \sum_{i=1}^{k} \sum_{j=i+1}^{k} \beta_{ij} X_j X_i \qquad (11)$$

Table 9. Experimental conditions applied for each run, in coded and in real values.

Run	Coded values				Experimental values			
	A	B	C	D	Tempera-ture (˚C)	Molar ratio MeOH/WCO (mol/mol)	Catatalyst Dosage (%wt)	Incorpora-tion of Oleic Acid (%wt)
1	1	1	0	0	65	15	1.4	1
2	0	0	1	-1	60	10	2.1	0
3	0	-1	0	1	60	5	1.4	2
4	0	-1	-1	0	60	5	0.7	1
5	0	1	1	0	60	15	2.1	1
6	0	1	-1	0	60	15	0.7	1
7	0	0	-1	1	60	10	0.7	2
8	1	0	0	-1	65	10	1.4	0
9	-1	0	0	-1	55	10	1.4	0
10	-1	1	0	0	55	15	1.4	1
11	0	0	0	0	60	10	1.4	1
12	-1	0	0	1	55	10	1.4	2
13	0	1	0	1	60	15	1.4	2
14	0	0	1	1	60	10	2.1	2
15	0	0	0	0	60	10	1.4	1
16	1	0	-1	0	65	10	0.7	1
17	0	1	0	-1	60	15	1.4	0
18	0	0	0	0	60	10	1.4	1
19	-1	-1	0	0	55	5	1.4	1
20	-1	0	-1	0	55	10	0.7	1
21	0	-1	0	-1	60	5	1.4	0
22	0	0	-1	-1	60	10	0.7	0
23	1	-1	0	0	65	5	1.4	1
24	-1	0	1	0	55	10	2.1	1
25	1	0	1	0	65	10	2.1	1
26	0	-1	1	0	60	5	2.1	1
27	1	0	0	1	65	10	1.4	2

5. RESULTS AND DISCUSSION

5.1 FEEDSTOCK CHARACTERIZATION

Biodiesel properties depend on the raw materials used, so it is important to characterize them. In this sense, waste cooking oil and oleic acid 90% were characterized by determining the acidity value, the FAME content by gas chromatography (GC-FID) and the FTIR analyses.

The acidity value of the raw materials was determined in triplicate, and the results are shown in Table 10.

Table 10. Acidity values of raw materials.

Sample	$Mass_{sample}$ (g)	V_{KOH} (mL)	C_{KOH} (mol/L)	AV (mg KOH/g)	$AV_{average}$ (mg KOH/g)	Standard deviation (mg KOH/g)
OA	1.0066	30.50	0.09450	160.63	160.81	0.1281
	1.0065	30.55		160.91		
	1.0065	30.55		160.90		
WCO	1.0027	0.24		1.27	1.22	0.0499
	1.0026	0.22		1.16		
	1.0024	0.24		1.27		

The initial acidity value found for the studied WCO sample was 1.22 mgKOH/gWCO. For the OA sample, the determined acid value was 160.81 mgKOH/gOA. Since the acid value is used to determine the amount of free fatty acids present in the oil samples and OA is a mixture of fatty acids (mainly oleic acid), the highest value found for the OA sample is consistent. Compared to WCO, OA has a higher acid value. Therefore, the introduction of controlled amounts of OA into the WCO samples allows the simulation of a highly acidic residual oil feedstock. These values were verified more than once, noting that they did not vary significantly over time, with a variation less than or equal to 1%.

The fatty acid of the raw materials was identified through the derivatization of the Fatty Acid Methyl Esters (FAME) by BF_3, and analysis by gas chromatography (GC-FID).

The chromatogram obtained for the derivatization of oleic acid is shown in Figure 12, in which the distribution of FAMEs formed can be qualitatively verified.

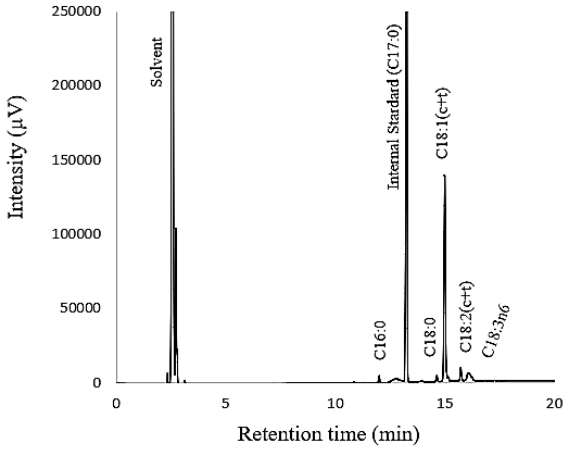

Figure 12. Chromatograms obtained by GC-FID for samples of oleic acid after derivatization.

Table 11 shows the amount of each FAME present in the oleic acid sample after its derivatization. It is possible to verify that the OA sample is constituted by 56.7% of oleic acid and elaidic acid, 13.8% of other fatty acids and 29.5% of unidentified compounds. The percentage of oleic acid present is lower than the 90% value described by the manufacturer.

Table 11. FAME profile obtained after derivatization of oleic acid.

Compound name	Compound ID	FAME (%)
Palmitic acid methyl ester	C16:0	1.4
Stearic acid methyl ester	C18:0	1.6
Oleic acid methyl ester, Elaidic acid methyl ester	C18:1 (c+t)	56.7
Linoleic acid methyl ester, Linolelaidic acid methyl ester	C18:2 (c+t)	3.7
gamma-Linolenic acid methyl ester	C18:3n6	7.1
Total		70.49

Figure 13 shows the chromatogram obtained by the derivatization of FAMEs from waste cooking oil. It is possible to verify that the presence of oleic acid methyl ester is lower in this case, but there is a greater presence of other FAMEs.

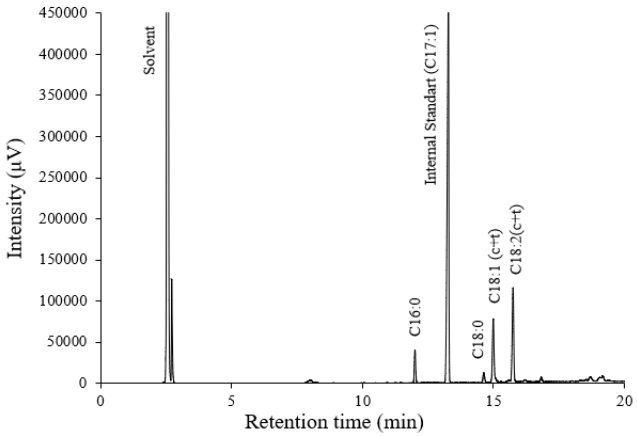

Figure 13. Chromatograms obtained by GC-FID for samples of waste cooking oil after derivatization.

The amount of each FAME present in the cooking oil waste sample after its derivatization can be seen in Table 12. It is observed that the WCO is constituted by 27.7% of linoleic acid and linolelaidic acid, 20.9% of acid oleic and elaidic acid, 8.1% palmitic acid, 3.0% stearic acid and 40.3% unknown compounds.

Table 12. FAME profile obtained after derivatization of waste cooking oil.

Compound name	Compound ID	FAME (%)
Palmitic acid methyl ester	C16:0	8.1
Stearic acid methyl ester	C18:0	3.0
Oleic acid methyl ester, Elaidic acid methyl ester	C18:1 (c+t)	20.9
Linoleic acid methyl ester, Linolelaidic acid methyl ester	C18:2 (c+t)	27.7
Total		59.70

FTIR analyses were performed for both samples. Fourier transform infrared spectroscopy analysis was used to identify the nature of the raw materials used in the production of biodiesel, verifying if there was the conversion of free fatty acids or triglycerides into esters.

Figure 14 shows the FTIR spectrum of oleic acid, used as a raw material in the production of biodiesel.

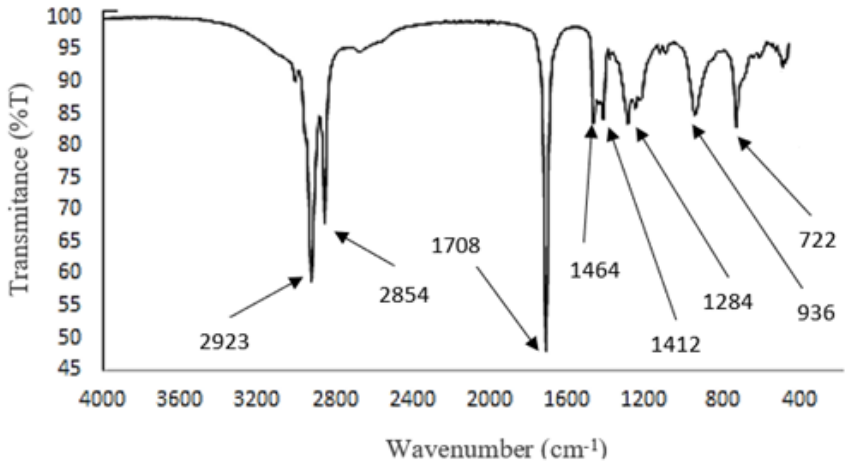

Figure 14. FTIR spectrum of oleic acid.

Carboxylic acids have a generally very wide band that occurs between 3400 and 2400 cm^{-1}, and centred at 3000 cm^{-1}, which represents an O-H bond strongly bonded by a hydrogen bond. This band normally overlaps the C-H absorptions. The 2923 and 2854 cm^{-1} bands that overlap the O-H bond are associated with the asymmetric and symmetrical elongation, respectively, of the aliphatic C-H bonds with sp^3 hybridization. The stretch C=O is also characteristic of carboxylic acids and occurs around 1730-1700 cm^{-1}. In the OA spectrum this band occurs at 1708 cm^{-1}, being the strongest and clearest band present in the spectrum. Band 1464 cm^{-1} corresponds to the folding of the CH_2 bond, and the band 1412 cm^{-1} to the folding of the C-O-H bond, which appears as a broad and weak peak between 1440 and 1220 cm^{-1}. C-O elongation, also characteristic of OA, usually occurs in the range of 1320 to 1210 cm^{-1}, with medium intensity. In this case, the connection appears at 1284 cm^{-1}. The band at 936 cm^{-1} is the result of an angular deformation to the plane of the O-H bond. The movement of rocks associated with four or more CH_2 groups in an open chain occurs at 720 cm^{-1}, appearing at 722 cm^{-1} in this sample [34, 37].

Figure 15 shows the FTIR spectrum of used cooking oil, one of the raw materials used in this work.

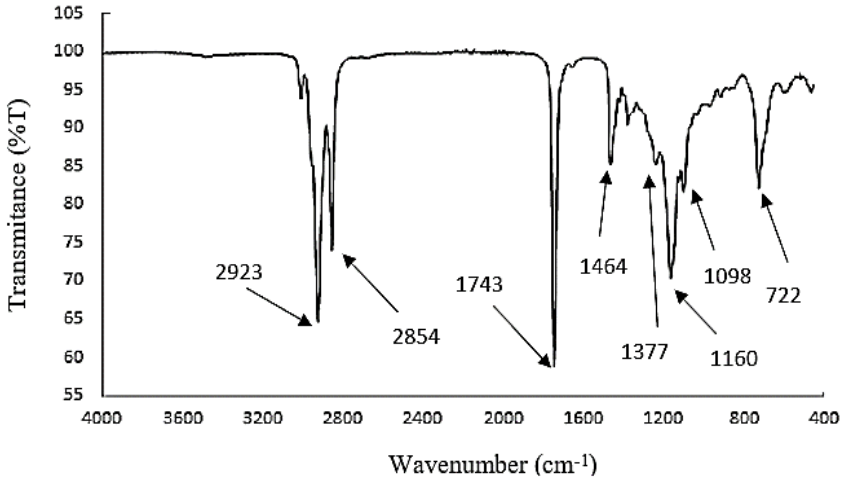

Figure 15. FTIR spectrum of waste cooking oil.

The oil is mainly composed of triglycerides, which are esters. As in the oleic acid spectrum, the 2924 and 2854 cm^{-1} bands correspond to the asymmetric and symmetrical elongation, respectively, of the aliphatic C-H bonds with sp^3 hybridization. The stretch C = O, also characteristic of esters, appears in the range from 1750 to 1735 cm^{-1}, occurring at 1743 cm^{-1} in this sample. The band 1464 cm^{-1} corresponds to the folding of the CH_2 bond, and the band 1377 cm^{-1}, to the folding of the CH_3 bond. The C-O stretch appears as two or more bands, one of the strongest and widest, in the range from 1300 to 1000 cm^{-1}. In this case, the link appears at 1160 and 1098 cm^{-1}. As seen also from the oleic acid spectrum, the rocking motion associated with four or more CH_2 groups in an open chain occurs at 722 cm^{-1} [34, 37].

5.2 CHOLINE HYDROXIDE

ChOH was purchased in a 45 wt.% methanol solution, so to confirm the concentration of the solution for the transesterification reaction, a titration was performed.

It was found out that the mass percentage of ChOH in the solution was 35.68%, and the titration data is shown in Table 13.

Table 13. Titration of ChOH(CH3OH) solution

Mass of ChOH(CH_3OH) Sample (g)	Volume HCl (mL)	n ChOH (mol)	Mass of ChOH (g)	ChOH Percentage	Average %ChOH
0.4002	12.80	1.1834×10^{-3}	0.1434	35.83	
0.4004	12.70	1.1742×10^{-3}	0.1423	35.53	35.68
0.4005	12.75	1.1789×10^{-3}	0.1429	35.67	

Figure 16 presents the FTIR obtained for the ChOH solution in methanol, which structure was previously shown in Figure 4. The band of greatest interest for biodiesel catalysis is the one designated by the OH stretch associated with hydrogen bond at 3278 cm^{-1}. The characteristic absorptions of choline hydroxide are those represented by the C-N bond and the $(CH_3)3N^+$ group of choline which are observed at 952 cm^{-1} and 1478 cm^{-1} respectively [41]. Besides, since this is a solution of choline hydroxide in methanol, the C-O stretching vibration appears in the spectrum at 1032 cm^{-1}. The peak at 2853 cm^{-1} is assigned relative to the stretching vibrations of symmetric and asymmetric aliphatic C-H in the CH_2 and the terminal CH_3 groups.

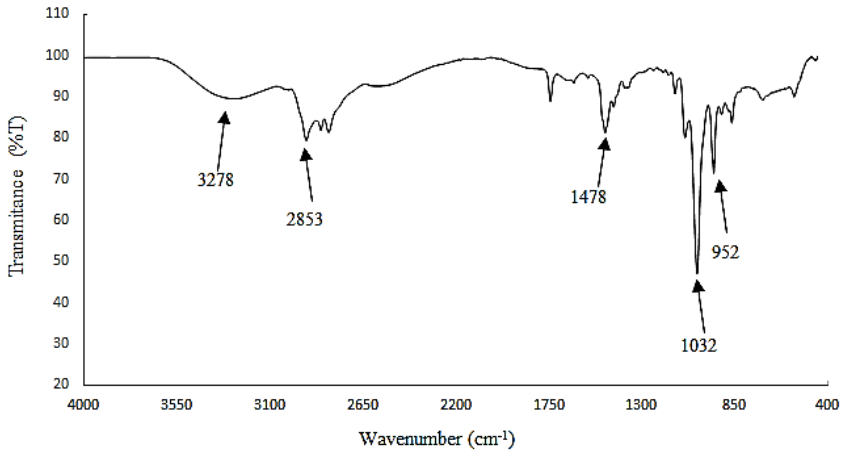

Figure 16. FTIR spectrum of choline hydroxide solution, 45 wt.% in methanol.

5.3 EXPERIMENTAL DESIGN

The optimization of the biodiesel production reaction was performed based on the Box Behnken Design (BBD), of four factors with three levels. From this method the combination matrix was determined with 27 runs. The parameters chosen as control factors were A: reaction temperature, B: molar ratio oil/methanol, C: percentage of catalyst and D: incorporation of oleic acid with all factors adjusted at three levels (-1, 0 and 1). Three response parameters were studied: R1, acidity value, R2, content in FAME and R3, the yield.

Table 14 describes the conditions applied in each run, both the design matrix and the actual values and their respective responses.

The evaluation of the responses was made separately. A different model was developed for each of the responses and different optimal conditions were estimated for the biodiesel production reaction. The acidity was determined by the analyses of the acidity of the biodiesel produced, according to the procedure described in section 4.4.1 The FAME content was determined by gas chromatography analysis of the biodiesel produced, according to the procedure in section 4.3.2. The yield was determined through the calculations of the mass of biodiesel produced, the % of FAME and the mass of the oil, also according to the procedure in section 4.3.2.

Table 14 shows that in run 26 there was no reaction, the cause could be that the fact that the ChOH catalyst is basic, and a neutralization reaction occurred when the catalyst was added at relatively small dosages, especially for artificially acidified oil samples. Therefore, the ChOH catalyst revealed high sensitivity towards the acidity of the oil.

Table 14. Experimental design, real conditions, and experimental responses.

Run	Experimental Design				Real Conditions				Experimental Responses		
	Temp. (˚C)	Molar Ratio WCO/MeOH	Cat. Dosage (%wt)	Incorp. OA(%wt)	Temp. (˚C)	Molar Ratio WCO/MeOH	Cat. Dosage (%wt)	Incorp. OA(%wt)	Acidity value (%)	FAME content (%)	Yield (%)
	A	B	C	D	A	B	C	D			
1	1	1	0	0	65	15	1.4	1	0.46	79.8	72.0
2	0	0	1	-1	60	10	2.1	0	0.83	60.1	48.6
3	0	-1	0	1	60	5	1.4	2	0.70	32.4	28.1
4	0	-1	-1	0	60	5	0.7	1	0.85	50.5	42.9
5	0	1	1	0	60	15	2.1	1	1.44	85.4	51.7
6	0	1	-1	0	60	15	0.7	1	0.85	6.1	5.4
7	0	0	-1	1	60	10	0.7	2	1.77	2.4	2.1
8	1	0	0	-1	65	10	1.4	0	0.46	60.5	51.6
9	-1	0	0	-1	55	10	1.4	0	0.88	60.1	52.5
10	-1	1	0	0	55	15	1.4	1	1.25	42.0	34.7
11	0	0	0	0	60	10	1.4	1	0.75	81.8	71.9
12	-1	0	0	1	55	10	1.4	2	1.74	22.1	17.1
13	0	1	0	1	60	15	1.4	2	1.35	73.0	51.2
14	0	0	1	1	60	10	2.1	2	0.67	28.7	24.2
15	0	0	0	0	60	10	1.4	1	0.74	82.8	73.7
16	1	0	-1	0	65	10	0.7	1	0.90	10.0	7.2
17	0	1	0	-1	60	15	1.4	0	0.99	79.9	69.0
18	0	0	0	0	60	10	1.4	1	0.74	79.0	69.6
19	-1	-1	0	0	55	5	1.4	1	0.90	54.5	48.0
20	-1	0	-1	0	55	10	0.7	1	0.90	9.7	8.7
21	0	-1	0	-1	60	5	1.4	0	0.79	61.8	52.9
22	0	0	-1	-1	60	10	0.7	0	0.66	23.2	20.7
23	1	-1	0	0	65	5	1.4	1	0.91	37.0	32.0
24	-1	0	1	0	55	10	2.1	1	1.34	37.9	27.9
25	1	0	1	0	65	10	2.1	1	0.60	23.8	19.8
26	0	-1	1	0	60	5	2.1	1	0.00	0.0	0.0
27	1	0	0	1	65	10	1.4	2	0.99	35.5	31.9

5.3.1 Analyses for the acidity value response

The analysis of variance (ANOVA) allows the comparison of the variation of the responses found for each combination of levels with the variation of the random errors associated to these responses. It considers the sources of imprecision and inaccuracy of the experiments. In this way it is possible to determine if the proposed regression is appropriate to the model [42].

Table 15 shows the ANOVA table for the acidity value of the biodiesel produced whose value was calculated with the aid of the software Experimental Design 11.

This value must be compared to the F-value tabulated (F test) by considering the degrees of freedom from both the regression and the residual. If the calculated value is higher than the tabulated one, means that the regression is statistically significant and therefore, the model is well fitted to the data, with a 95% confidence level. In the current analysis, the calculated F-value for the regression is 5.38. Considering the degrees of freedom of the regression (df1 = 14) and the degrees of freedom of the residual (df2 = 12) and checking the Fisher's distribution table for the critical value of $F_{14,12,0.05}$ (α equal to 0.05), it is possible to find a tabulated value of 2.64. The calculated value is higher than the tabulated, indicating a reliable model.

As it can be seen on Table 15, the calculated F-value is higher than the tabulated one for the following parameters: A (temperature), B (molar ratio), AB, BC, and CD. The remaining terms are not significant, including, in this list, the catalyst dosage (C) and incorporation of OA (D). Besides helping to understand whether the factor is statistically significant, the ANOVA helps to interpret how significant each one is. This can be assessed by the *p-value*. The lowest it is, the highest the influence on the response. In this way, the order of importance is A > B > BC > CD >AB > D.

Table 15. ANOVA analysis for the parameters influencing the acidity value.

Source	Sum of Squares	df*	Mean square	Calculated F-value	Tabulated F-value	p-value
Model	3.46	14	0.2470	5.38	2.64	3×10^{-3}
A-Temperature	0.8696	1	0.8696	18.93	4.75	9×10^{-4}
B-Molar Ratio	0.8101	1	0.8101	17.64	4.75	1.2×10^{-3}
C- Catalyst Dosage	0.0412	1	0.0412	0.8966	4.75	0.3624
D-Incorporation OA	0.2176		0.2176	4.74	4.75	0.0502
AB	0.2550	1	0.2550	5.55	4.75	0.0363
AC	0.1369	1	0.1369	2.98	4.75	0.1099
AD	0.0169	1	0.0169	0.3679	4.75	0.5554
BC	0.5184	1	0.5184	11.29	4.75	0.0057
BD	0.0506	1	0.0506	1.10	4.75	0.3145
CD	0.4032	1	0.4032	8.78	4.75	0.0119
A^2	0.1070	1	0.1070	2.33	4.75	0.1528
B^2	0.0042	1	0.0042	0.0905	4.75	0.7687
C^2	0.0093	1	0.0093	0.2016	4.75	0.6614
D^2	0.1688	1	0.1688	3.68	4.75	0.0793
Residual	0.5512	12	0.0459			
Lack of Fit	0.5511	10	0.0551	1653.37	19.40	6×10^{-4}
Pure error	0.0001	2	0			
Cor Total	4.01	26				

df*= Degree of freedom

Another way to evaluate the model is to check for lack of fit. As with the regression fit, the lack of fit must be evaluated by comparing the calculated F value with the tabulated value. In this case, the degrees of freedom of lack of fit and pure error must be considered. The F distribution points out that, for an $F_{10,2,0.05}$, the value is 19.40, while the calculated F value is 1653.37, which means that the lack of fit is significant. This is not the expected response to lack of adjustment. This means that the model errors are due to a problem of fitting the data.

The p-value is related to the F-value and is defined as the probability that the data are at least as extreme as observed [43]. In other words, it is related to the strength of the evidence against the null hypothesis. Low p-values allow rejecting the null hypothesis, which in this case would be that the model is not relevant or that the factors do not influence the answer. If the null hypothesis is rejected, then the alternative hypothesis must be true, which would mean that the model and factors are relevant. Treatments that result in p-values below a predetermined level of significance, which in this case is 0.05, are considered statistically significant. Therefore, the current model is statistically relevant, and

the lack of adjustment is not relevant, that is, in the adjustment, the factors do not influence the response.

5.3.1.1 Residuals analyses for acidity value

The quality of fit was also assessed by analysing the coefficient of determination, which was estimated at R^2 = 0.8625 and R^2 adjusted = 0.7021. The proximity of these values indicates the non-occurrence of residuals in the analysis, as the residuals are the subtraction of the observed response from the expected response. The expectation is that the data will normally be distributed within a straight diagonal line, with no residuals occurring too far from the line. There are no outliers, that is, discrepant points that affect the adequacy of the model to the experimental data. Figure 17 (A) shows the set of experimental data in question, normally distributed.

The residues versus predicted plotted in Figure 17 (B) help to verify that the residues approach the null value and that the residues follow a specific standard. In this case the graph within the expected patterns because the points are near the centerline. Another important aspect of this tool is to assist in the identification of outliers, which are runs which exhibit very large residuals that must be discarded from the statistical evaluation, that is, any value outside the red line must be considered an outlier and the experiment or response measurements must be repeated.

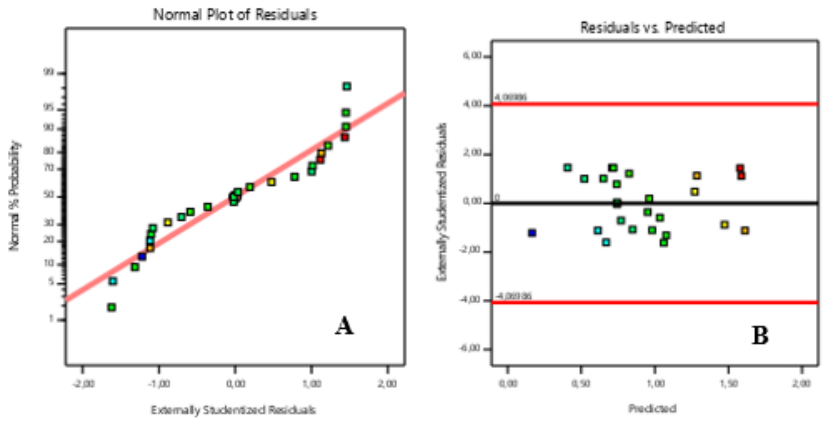

Figure 17. Normal plot of residuals for the acidity value (**A**); Residual versus predicted for the acidity value(**B**).

5.3.1.2 Effect of the factors on the acidity value

Figure 18 through 23, show the response surface for several pairs of parameters and the interaction plots of those same variables and their influence on the acidity value, experimental values. Any variable that is not on displayed in each plot has been set to its intermediate value.

Figure 18 shows the response surface relating to the influence of the variables: temperature (A) and molar ratio WCO/methanol (B), and the interaction graph for these two variables.

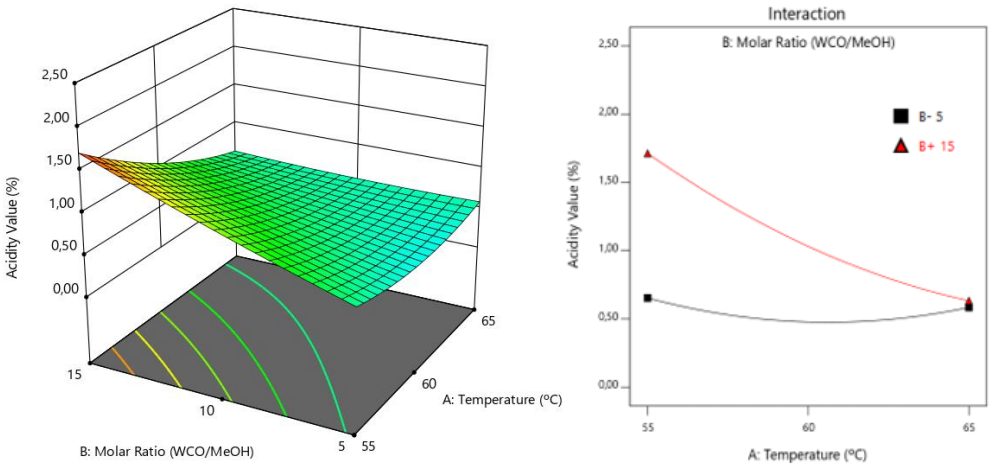

Figure 18. Response surface regarding the influence of temperature (A) and molar ratio WCO/methanol (B) on the acidity value and the interaction plot of those variables.

The response surface indicates that variable A has a great influence on the acidity results. By observing the values along the axis, A at a fixed point at B, can be observed a significant variation in the slope between the factor levels. Analysing now the variation in the slope of the straight lines in relation to the B axis, it also observed a great variation between the values obtained at the studied levels. What is also evident is that factor A has a negative effect on the response and factor B has a positive effect, as the slopes of the lines between the levels for each of these factors present the opposite behavior, the first decreases while the second increases.

In the Figure 18 the lines that associate variables A and B are not parallel lines, it means that the effect displayed by one factor depends on the level of the other factor. In other words, it means that one factor not only influences the response by itself, but it also influences the other variable, changing the effect of this second variable on the response.

The existence of this interaction is confirmed by the analysis of the p-value determined in ANOVA, where the AB interaction has significance for the appropriate model.

Figure 19 shows the response surface with respect to the influence of the variables: temperature (A) and catalyst dosage (C), and the interaction graph of these two variables.

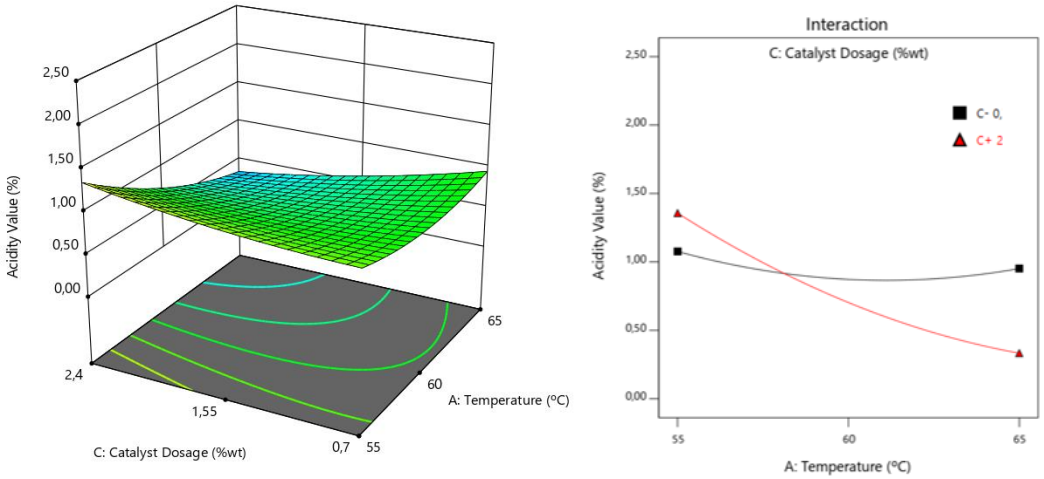

Figure 19. Response surface regarding the influence of temperature (A) and catalyst dosage (C) on the acidity value and the interaction plot of those variables.

The response surface indicates that for low values of variables A and C there is no great influence on the acidity results. Observing the values along the axis, A at a fixed point in C, there is no significant variation in the slope between the levels of the factors, the same happens for the variable C. Analysing now, higher values of the variables, a variation in the slope of the straight lines in relation to the axes, it can be observed. This makes it clear that factors A and C have a negative effect on the response.

The interaction graph factors A and C shows two non-parallel lines representing the interaction between the factors to the studied response, that is, the effect caused by the change in the level of factor A in the response is dependent of the level of factor C and vice versa.

Figure 20 shows the response surface in relation to the influence of the variables: temperature (A) and incorporation of OA (D) and the interaction graph of these two variables.

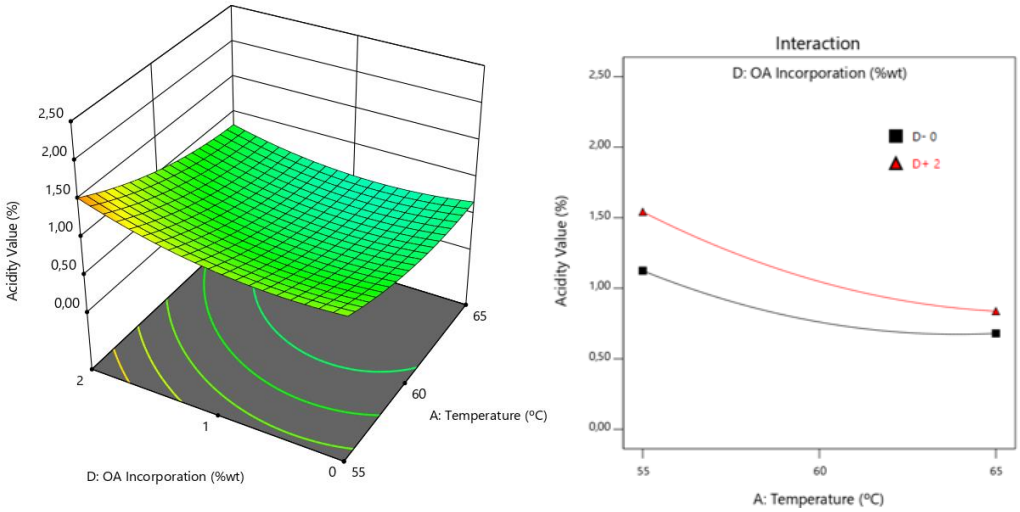

Figure 20. Response surface regarding the influence of temperature (A) and incorporation of oleic acid (D) on the acidity value and the interaction plot of those variables.

The response surface indicates that the D factor has influence on the acidity value response. When analysed the factor A, the acidity value response hardly changes along the A axis between levels. Therefore, it is concluded that factor D has a greater influence on the acidity value response than factor A.

The interaction plot of factors A and D shows two lines practically parallel which represent the absence of interaction between the factors in the response, that is, the effect caused by the change in the factor A level in the response is independent of the factor level D and vice versa. It is confirmed the non-existence of this interaction by the analysis of the p-value determined in ANOVA, where the interaction AD has no significance for the model developed.

Figure 21 shows the response surface in relation to the influence of the variables: molar ratio WCO/ methanol (B) and catalyst dosage (C) and the interaction graph of these two variables.

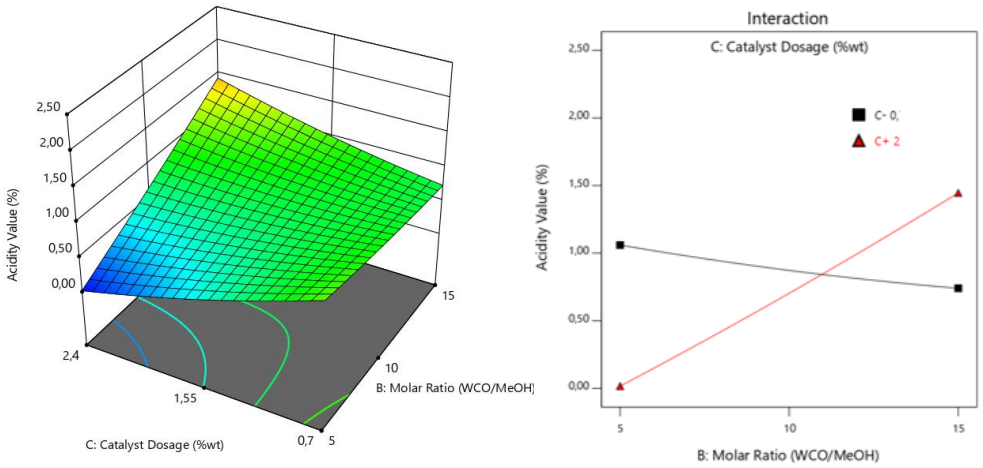

Figure 21. Response surface regarding the influence of molar ratio WCO/MeOH (B) and catalyst dosage (C) on the acidity value and the interaction plot of those variables.

The response surface indicates that each variable has a great influence on the acidity results. Analysing the variation in the slope of the straight lines in relation to the C axis, a large variation can be observed between the values obtained at the levels studied. What is also evident is that for low B axis values, the C factor has a negative effect, and for high B values it has a positive effect on the response. While factor B has a positive effect on the response along the entire C axis.

The interaction graph factors B and C shows two non-parallel lines representing the interaction between the factors to the studied response, that is, the effect caused by the change in the level of factor B in the response is dependent of the level of factor C and vice versa.

Figure 22 shows the response surface in relation to the influence of the variables: molar ratio WCO/ methanol (B) and incorporation of oleic acid (D) and the interaction graph of these two variables.

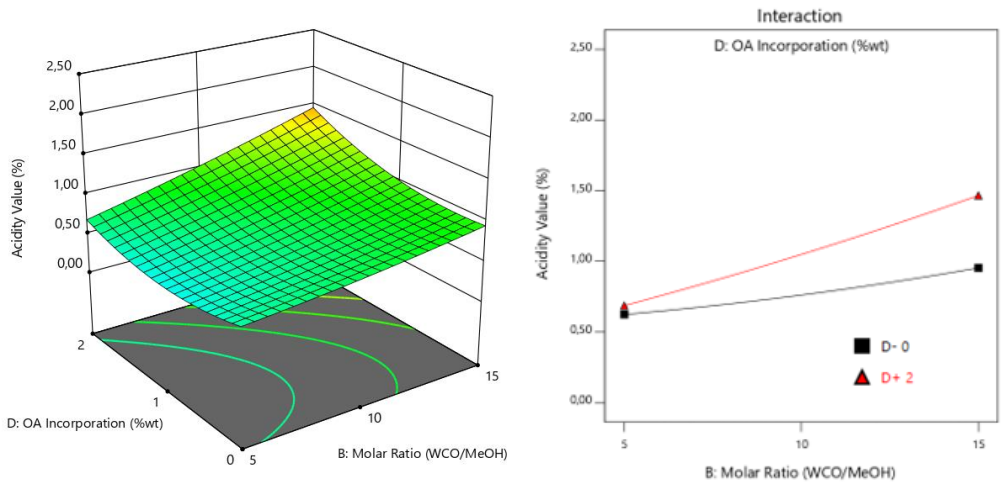

Figure 22. Response surface regarding the influence of molar ratio WCO/MeOH (B) and incorporation of oleic acid (D) on the acidity value and the interaction plot of those variables.

The response surface indicates that the B factor has a great influence on the acidity value response. While for the factor D, the acidity value response hardly changes along the B axis between levels. Therefore, the factor B has a greater influence on the acidity value response than factor D.

The interaction graph factors B and D shows two non-parallel lines representing the interaction between the factors to the studied response, that is, the effect caused by the change in the level of factor B in the response is dependent of the level of factor C and vice versa.

Figure 23 shows the response surface in relation to the influence of the variables: catalyst dosage (C) and incorporation of oleic acid (D) and the interaction graph of these two variables.

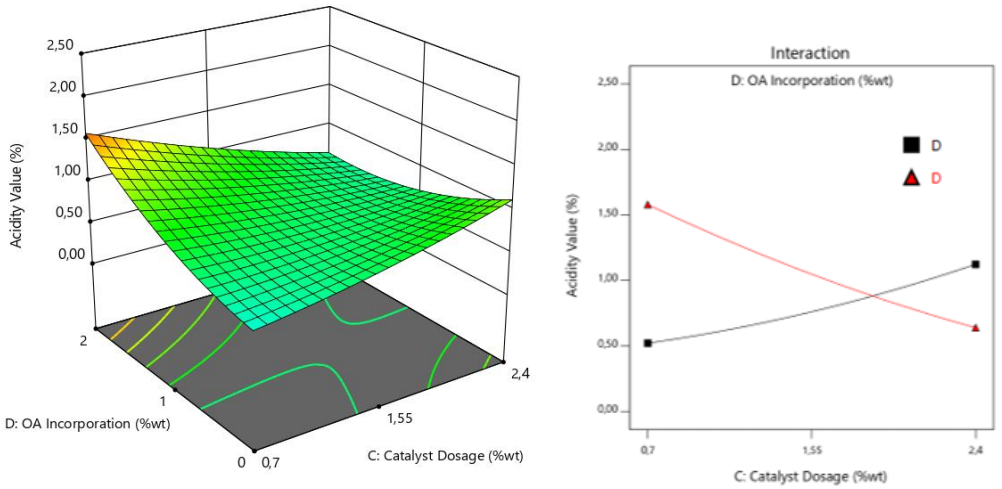

Figure 23. Response surface regarding the influence of catalyst dosage (C) and incorporation of oleic acid (D) on the acidity value and the interaction plot of those variables (A= 0; B = 0).

The response surface indicates that variable C, has a great influence on the conversion results. Analysing the slope variation in the lines concerning the D axis, a great variation between the values obtained between the studied levels is also observed. What is also evident is that factor C has a negative effect for higher D and a positive effect for lower D on the response. On the other hand, fact D has a positive effect on the lower C and a negative effect on the upper C in the response.

The interaction graph factors C and D shows two non-parallel lines representing the interaction between the factors to the studied response, that is, the effect caused by the change in the level of factor C in the response is dependent of the level of factor D and vice versa.

5.3.1.3 Mathematical model for acidity value

Table 16 shows the coefficients determined for the mathematical model constructed through the regression of the experimental data corresponding to the acidity value response. From the calculated coefficients, it is possible to build the equation that best fits the total factor studied. This model represents how the studied factors, and their interactions influence the acidity value response. The model equation is represented by Equation (11).

Table 16. Coefficients for acidity value.

Coded factor	Coefficient
Intercept	0.7265
A	-0.2871
B	0.2771
C	-0.0846
D	0.1436
AB	-0.2525
AC	-0.2246
AD	-0.0650
BC	0.4371
BD	0.1125
CD	-0.3855
A^2	0.1417
B^2	0.0279
C^2	0.0614
D^2	0.1779

$$Y = 0.7265 - 0.2871A + 0.2771B - 0.0846C + 0.1436D - 0.2525AB - 0.2246AC - 0.0650A + 0.4371BC + 0.1125BD - 0.3855CD + 0.1417A^2 + 0.0279B^2 + 0.614C^2 + 0.1779D^2 \quad (12)$$

In the Equation (12), factor A, C and the interaction AB, AC, AD, CD and have a negative effect on the response, while factors B, D and other interactions have positive effects.

5.3.1.4 Optimum conditions for the acidity value

By minimizing Equation (12), it is possible to determine which values for the set of parameters studied would lead to the highest acidity value, which is shown in Table 17, both in real values. It is important to understand that the optimal values found are strongly related to the region studied. If the actual values of the molar ratio were changed, for example, possibly the optimal combination of parameters would be different.

Table 17. Optimal conditions for acidity value.

Factor	ID factor	Optimum value
A	Temperature	63 ºC
B	Molar ratio WCO /MeOH	1:13 (mol/mol)
C	Catalyst Dosage	1.5 %
D	Incorporation of OA	0.5 %

According to these conditions to have acidity value of 0.6, a FAME content of 85.4% and a yield of 73.7% is requires, for a confidence level of 95%.

5.3.2 Analyses for FAME content

Analysis of variance (ANOVA) was performed to assess the importance of the model. The ANOVA results were within the 95% confidence interval used to validate the model. Response and interaction surface graphs were presented to visualize the process variables in methyl ester content.

From the ANOVA, it is possible to notice the significance of the model obtained for the FAME content response, when comparing the calculated F, which has the value 31.77, and the tabulated F, which is equal to 2.64. Thus, $F_{calculated} > F_{tabulated}$ denoting the fit of the model. Comparing the p-value of the model of <0.0001 with the alpha assigned to 0.05 reaffirms the significance of the model, since p <value of α. Thus, the regression is statistically significant and, therefore, the model fits well to the experimental data, with a confidence level of 95%.

Regarding the lack of adjustment, the comparison between $F_{tabulated}$, which presents a value of 19.40, with a calculated F of 13.57 indicates its non-significance, since $F_{tabulated} > F_{calculated}$, that is, the model errors are due to the random and inherent system errors and do not relate to problems with data fit. This conclusion reaffirms that for the FAME content response, the model is significant, while the lack of fit is not.

For the analysis of variance of the response to FAME content, the significant factors are B (oil/methanol molar ratio), D (incorporation of OA), D^2 interactions AB, BC, A^2, C^2 and D^2, while the factors A(temperature), C (catalyst dosage) and the AC and BC and B^2 interactions are not significant.

Table 18 shows the ANOVA table for the FAME content whose value was calculated with the aid of the software Experimental Design 11.

Table 18. Analysis of variance for the fitted quadratic model for FAME content.

Source	Sum of Squares	df	Mean square	Calculated F-value	Tabulated F-value	p-value
Model	19276.36	14	1376.88	31.77	2.64	$<1\times10^{-4}$
A-Temperature	9.01	1	9.01	0.2078	4.75	0.6566
B-Molar Ratio	3334.70	1	3334.70	76.93	4.75	$<1\times10^{-4}$
C- Catalyst Dos-age	263.08	1	263.08	6.07	4.75	0.0298
D-Incorporation OA	1834.94		1834.94	42.33	4.75	$<1\times10^{-4}$
AB	765.35	1	765.35	17.66	4.75	1.2×10^{-3}
AC	51.77	1	51.77	1.19	4.75	0.2959
AD	41.86	1	41.86	0.9658	4.75	0.3451
BC	4215.26	1	4215.26	97.25	4.75	$<1\times10^{-4}$
BD	125.66	1	125.66	2.90	4.75	0.1144
CD	28.30	1	28.30	0.6530	4.75	0.4348
A^2	2618.52	1	2618.52	60.41	4.75	$<1\times10^{-4}$
B^2	190.11	1	190.11	4.39	4.75	0.0581
C^2	8138.19	1	8138.19	187.76	4.75	$<1\times10^{-4}$
D^2	1019.06	1	1019.06	23.51	4.75	4×10^{-4}
Residual	520.14	12	43.34			
Lack of Fit	512.58	10	51.26	13.57	19.40	0.0705
Pure error	7.55	2	3.78			
Cor Total	19796.49	26				

df*= Degree of freedom

5.3.2.1 Analyses of residuals for FAME content

Residual analysis is presented in the normal probability graph in Figure 24(A). The FAME content response data are normally distributed, spread very close to the diagonal line, indicating that the constructed model is reliable and meaningful. The coefficient of determination was estimated at $R^2 = 0.9737$ and the adjusted $R^2 = 0.9431$, which reinforces the fact that there is a good regression.

The Residuals vs. Predicted Values is shown in Figure 24(B) and allows verifying that the residuals are independent of the level of known variables and are distributed close to line 0, inside the red lines, not showing outliers. These data reveal the good statistical quality of the data and the adequacy of the estimated mathematical model.

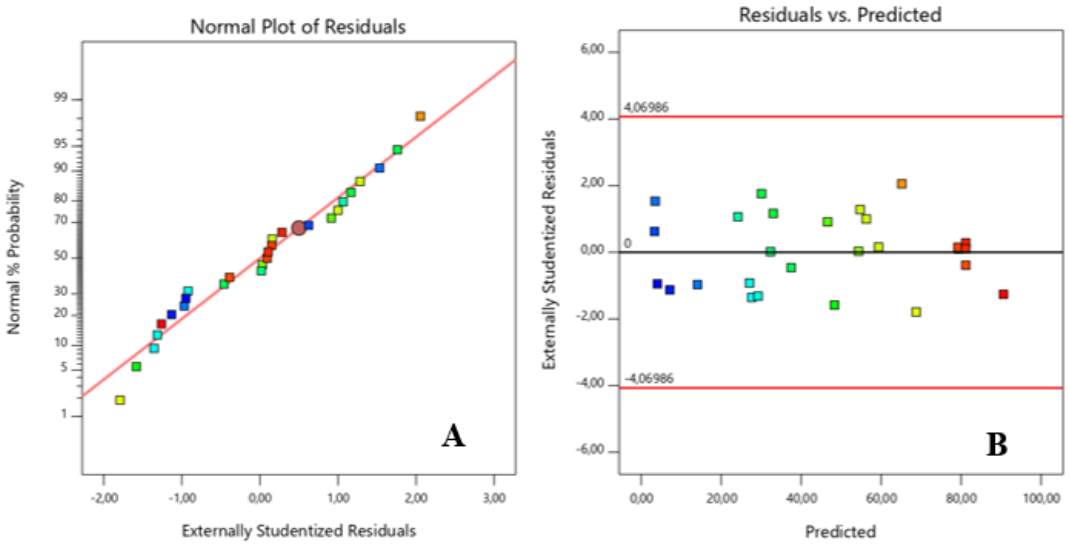

Figure 24. Normal plot of residuals for the FAME content (**A**); Residual versus predicted for the FAME content (**B**).

5.3.2.2 Factors effect on the FAME content

Figure 25 shows the response surface in relation to the influence of the variables: temperature (A) and molar ratio WCO/methanol (B), and the interaction graph for these two variables.

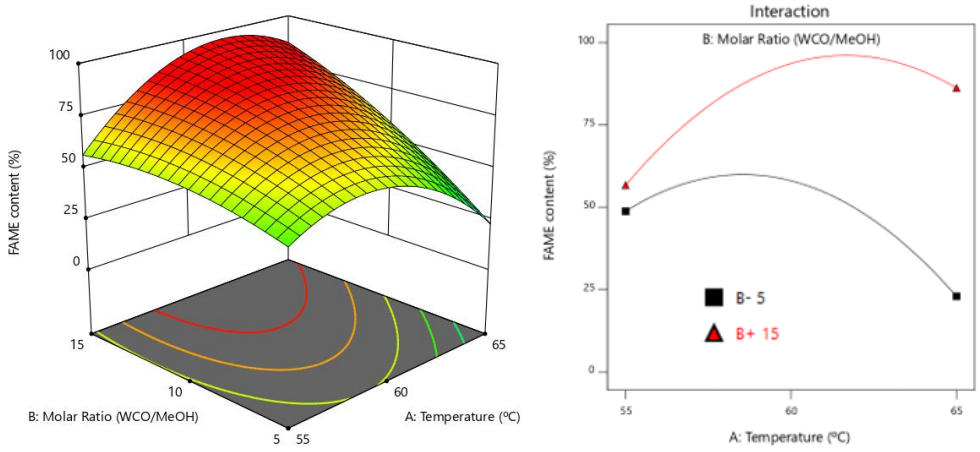

Figure 25. Response surface regarding the influence of temperature (A) and molar ratio WCO/MeOH (B) on the FAME content and the interaction plot of those variables.

Performing the analysis, it is possible to see that the response surface indicates that the variable A has a great influence on the FAME content results, since there is variation between the levels of the factors. On the other hand, for variable B it is possible to verify that the response increases significantly when the levels of factors vary. Thus, factors A and B have greater influence on the FAME content response and have a positive effect on the response.

The interaction graph factors A and B shows two non-parallel lines representing the interaction between the factors to the studied response, that is, the effect caused by the change in the level of factor A in the response is dependent of the level of factor B and B depend on factor A. It is confirmed the existence of this interaction by the analysis of the p-value determined in ANOVA, where the interaction AB has significance for the model developed.

Figure 26 shows the response surface in relation to the influence of the variables: temperature (A) and catalyst dosage (C), and the interaction graph for these two variables.

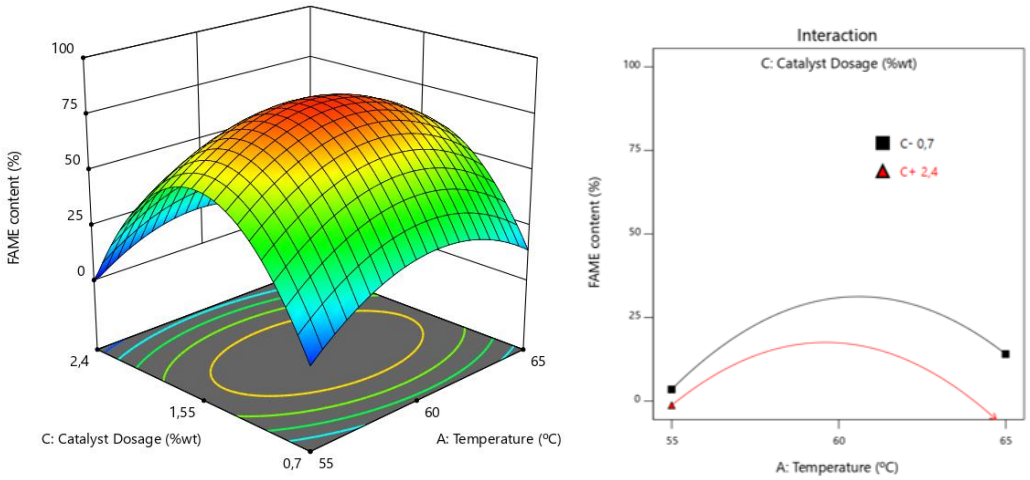

Figure 26. Response surface regarding the influence of temperature (A) and catalyst dosage (C) on the FAME content and the interaction plot of those variables.

The response surface indicates that the C factor has a great influence on the FAME content, as observing the surface along the C axis at a fixed point in A, there is a significant variation. There is a big difference in the slopes corresponding to the two factors. When the same analysis is done for the A factor, the FAME content response also changes along the A axis between levels. Therefore, it is concluded that factor A and C has a great influence on the FAME content response.

The interaction graph factors A and C shows two non-parallel lines representing the interaction between the factors to the studied response, that is, the effect caused by the change in the level of factor A in the response is dependent of the level of factor C and vice versa.

Figure 27 shows the response surface in relation to the influence of the variables: temperature (A) and incorporation of OA (D), and the interaction graph for these two variables.

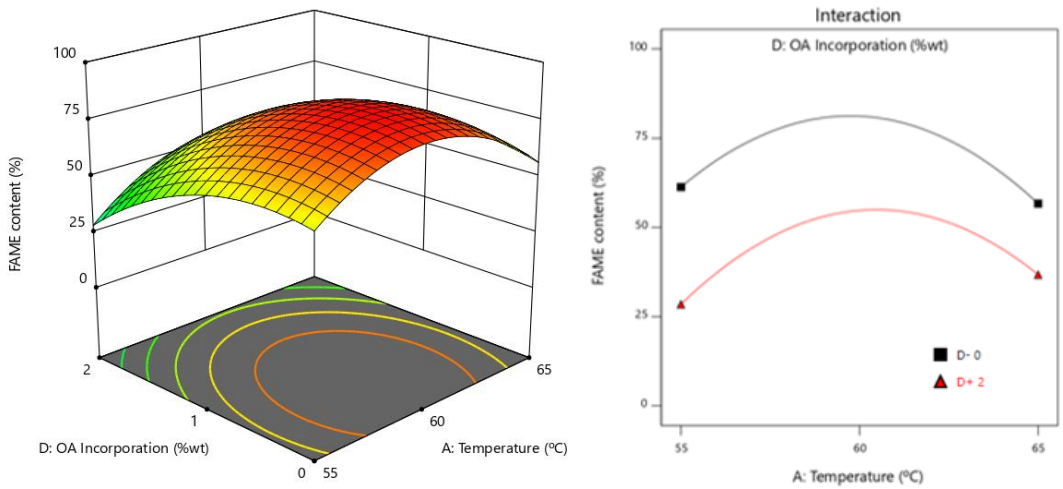

Figure 27. Response surface regarding the influence of temperature (A) and incorporation of oleic acid (D) on the FAME content and the interaction plot of those variables.

The response surface indicates that variables A and D have a great influence on the results. However, the smaller the D factor, the greater the effect on the FAME content response. For the A factor, the FAME content response changes slightly along the A axis between levels.

The interaction graph factors A and D shows two non-parallel lines representing the interaction between the factors to the studied response, that is, the effect caused by the change in the level of factor A in the response is dependent of the level of factor D and vice versa.

Figure 28 shows the response surface in relation to the influence of the variables: molar ratio WCO/MeOH (B) and catalyst dosage (C), and the interaction graph for these two variables.

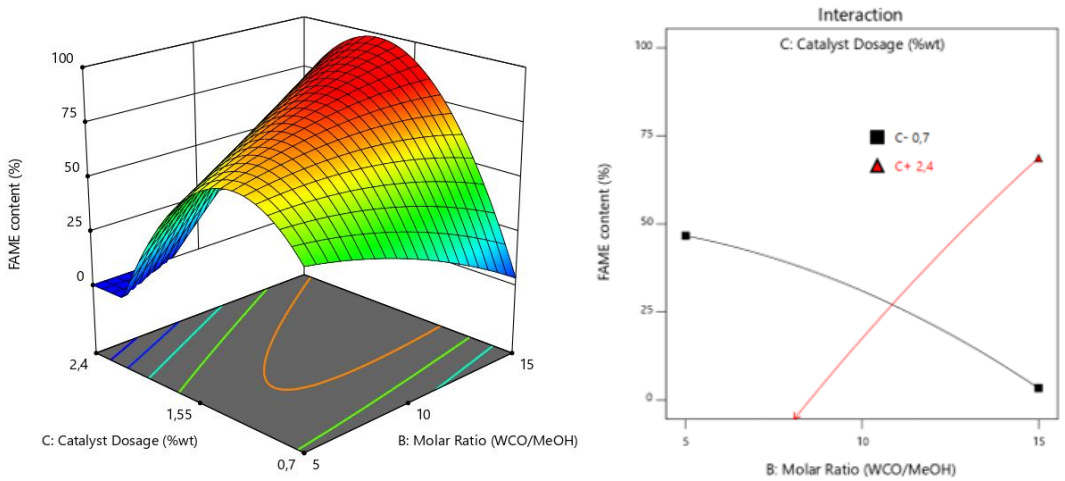

Figure 28. Response surface regarding the influence of molar ratio WCO/MeOH (B) and catalyst dosage (C) on the FAME content and the interaction plot of those variables.

The response surface indicates that variable B has a great influence on the FAME content results. Analysing the variation of the inclination in the straight lines in relation to the C axis, it is also observed a great variation between the values obtained between the levels studied.

The interaction graph factors B and C shows two non-parallel lines representing the interaction between the factors to the studied response, that is, the effect caused by the change in the level of factor B in the response is dependent of the level of factor C and vice versa.

Figure 29 shows the response surface in relation to the influence of the variables: molar ratio of WCO/MeOH (B) and incorporation of oleic acid (D) and the interaction graph for these two variables.

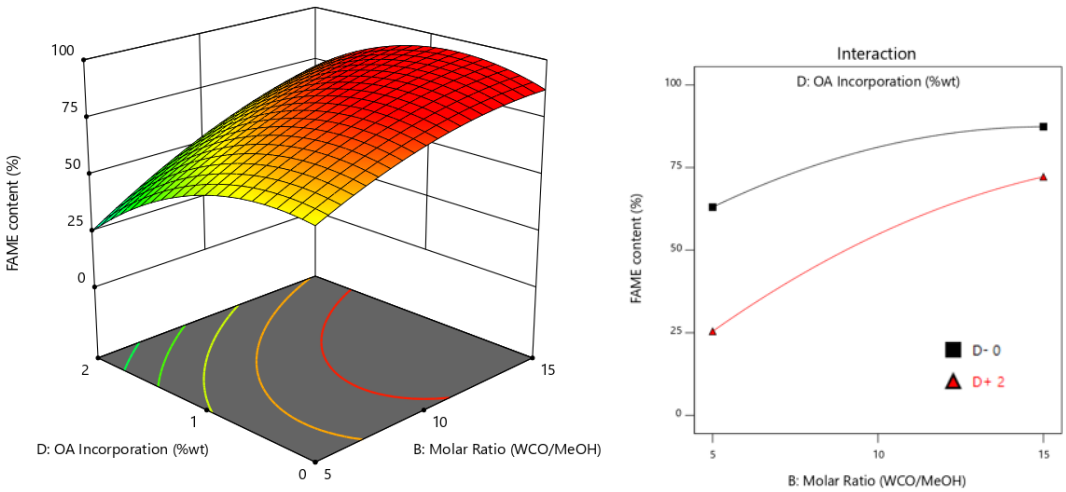

Figure 29. Response surface regarding the influence of molar ratio WCO/MeOH (B) and incorporation of oleic acid (D) on the FAME content and the interaction plot of those variables.

The response surface indicates that variables B and D have a great influence on the results. However, the smaller the D factor, the greater the effect on the FAME content response. For factor B, the longer axis A, the greater the FAME results.

The interaction plot of factors B and D shows two lines practically parallel which represent the absence of interaction between the factors in the response, that is, the effect caused by the change in the factor B level in the response is independent of the factor level D and vice versa. It is confirmed the non-existence of this interaction by the analysis of the p-value determined in ANOVA, where the interaction BD has no significance for the model developed.

Figure 30 shows the response surface in relation to the influence of the variables: catalyst dosage (C) and incorporation of oleic acid (D)and the interaction graph for these two variables.

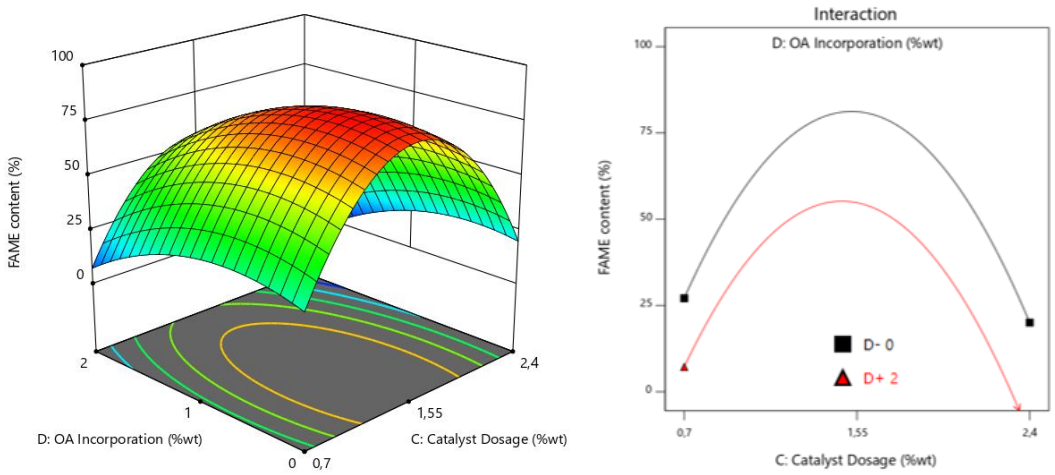

Figure 30. Response surface regarding the influence of catalyst dosage (C) and incorporation of oleic acid (D) on the FAME content and the interaction plot of those variables.

The response surface indicates that variable C and D has a great influence on the FAME content results. Analysing the variation of the inclination in the straight lines in relation of the axis, it is also observed a great variation between the values obtained between the levels studied.

The interaction graph factors C and D shows two non-parallel lines representing the interaction between the factors to the studied response, that is, the effect caused by the change in the level of factor C in the response is dependent of the level of factor D, on the other hand the factor D depends on the factor C.

5.3.2.3 Mathematical model for the FAME content

Table 19 shows the coefficients determined for the mathematical model constructed through the regression of the experimental data corresponding to the FAME content response. From the calculated coefficients, it is possible to build the equation that best fits the total factor studied. This model represents how the studied factors, and their interactions influence the FAME content response. The model equation is represented by Equation (12).

Table 19. Coefficients for FAME content.

Coded factor	Coefficient
Intercept	81,79
A	0,9241
B	17,78
C	-6,76
D	-13,19
AB	13,83
AC	-4,37
AD	3,24
BC	39,42
BD	5,61
CD	-3,23
A^2	-22,16
B^2	-5,97
C^2	-57,6
D^2	-13,82

$$Y = 81.79 + 0.9242A + 17.78B - 6.76C - 13.19D + 13.83AB - 4.37AC + 3.24AD + 39.42BC + 5.61BD - 3.23CD \pm 22.16A^2 \pm 5.97B^2 - 57.60C^2 - 13.82D^2 \quad (13)$$

In Equation (13) factors A, B and interactions AB, AD, BC, and BD have a positive effect on the response, while factor C, D and other interactions have a negative effect.

5.3.2.4 Optimal conditions for FAME content

For the studied conditions, factors, and their respective contents, it was possible to determine the best conditions to obtain the maximum FAME content from the waste cooking oil. The best conditions with coded and actual values are shown in Table 20.

Table 20. Best conditions for FAME content.

Factor	ID factor	Optimum value
A	Temperature	63ºC
B	Molar ratio WCO /MeOH	1:13 (mol/mol)
C	Catalyst Dosage	1.5 %
D	Incorporation of OA	0.5 %

According to these conditions, to have a FAME content of 85.4%, an acidity value of 0.61 and a yield of 73.7% is required for a confidence level of 95%.

5.3.2.5 Analyses for the yield

The ANOVA table was built the same way it was built for the FAME content. The ANOVA for the evaluation of yield presented in Table 21 indicates that the model is

significant, with a calculated F value greater than the tabulated one. Also, the lack of adjustment is not significant (calculated F value lower than tabulated).

For the analysis of variance of the yield response, the significant factors are B, C, D and interaction AB, BC, A^2, B^2, C^2 and D^2 while the factors A and other interactions are not significant.

Table 21. Analysis of variance for the fitted quadratic model for yield.

Source	Sum of Squares	df	Mean square	Calculated F-value	Tabulated F-value	p-value
Model	13323.76	14	951.70	19.98	2.64	1×10^{-4}
A-Temperature	33.58	1	33.58	0.7050	4.75	0.4175
B-Molar Ratio	1383.27	1	1383.27	29.04	4.75	3×10^{-4}
C- Catalyst Dosage	638.89	1	638.89	13.41	4.75	3.3×10^{-3}
D-Incorpora-tion OA	1526.84		1526.84	32.05	4.75	1×10^{-4}
AB	709.55	1	709.55	14.90	4.75	2.3×10^{-3}
AC	10.86	1	10.86	0.2280	4.75	0.6416
AD	61.26	1	61.26	1.29	4.75	0.2789
BC	1990.69	1	1990.69	41.79	4.75	$<1\times10^{-4}$
BD	12.44	1	12.44	0.2611	4.75	0.6168
CD	8.42	1	8.42	0.1768	4.75	0.6816
A^2	1883.22	1	1883.22	39.53	4.75	$<1\times10^{-4}$
B^2	360.71	1	360.71	7.57	4.75	0.0175
C^2	7226.25	1	7226.25	151.70	4.75	$<1\times10^{-4}$
D^2	897.73	1	897.73	18.85	4.75	1×10^{-3}
Residual	571.62	12	47.63			
Lack of Fit	563.17	10	56.32	13.33	19.40	0.0717
Pure error	8.45	2	4.22			
Cor Total	13895.38	26				

df*= Degree of freedom

5.3.2.6 Analyses of residuals for the Yield

Residual analysis is presented in the normal probability graph in Figure 31(A). The yield response data are normally distributed, spread very close to the diagonal line, indicating that the constructed model is reliable and meaningful. The coefficient of determination was estimated at $R^2 = 0.9589$ and the adjusted $R^2 = 0.9109$, which reinforces the fact that there is a good regression.

The Residuals vs. Predicted Values is shown in Figure 31(B) and allows verifying that the residuals are independent of the level of known variables and are distributed close

to line 0, inside the red lines, not showing outliers. These data reveal the good statistical quality of the data and the adequacy of the estimated mathematical model.

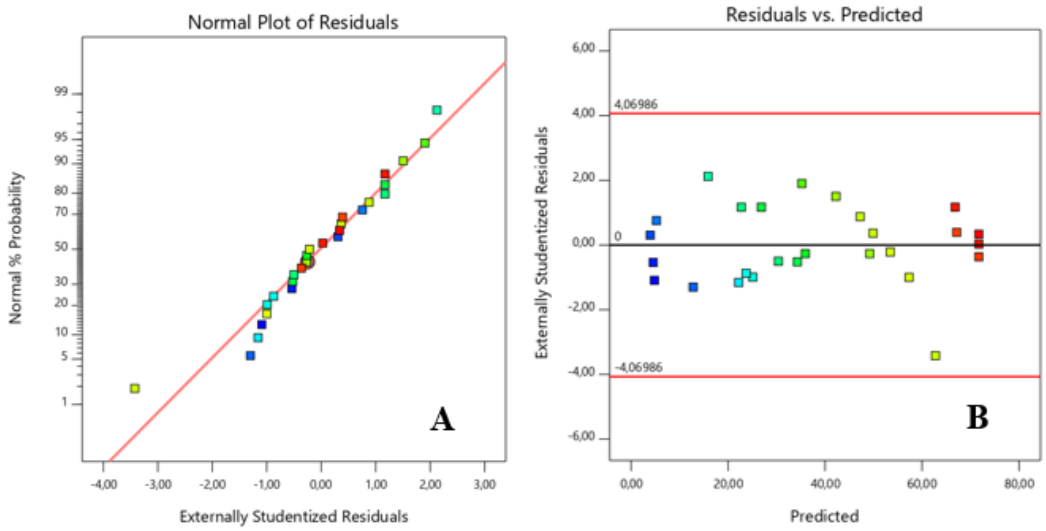

Figure 31. A: Normal plot of residuals for the yield; B: Residual versus predicted for the yield.

5.3.2.7 Factors effect on yield

Figure 32 shows the response surface in relation to the influence of the variables: temperature (A) and molar ratio WCO/methanol (B), and the interaction graph for these two variables.

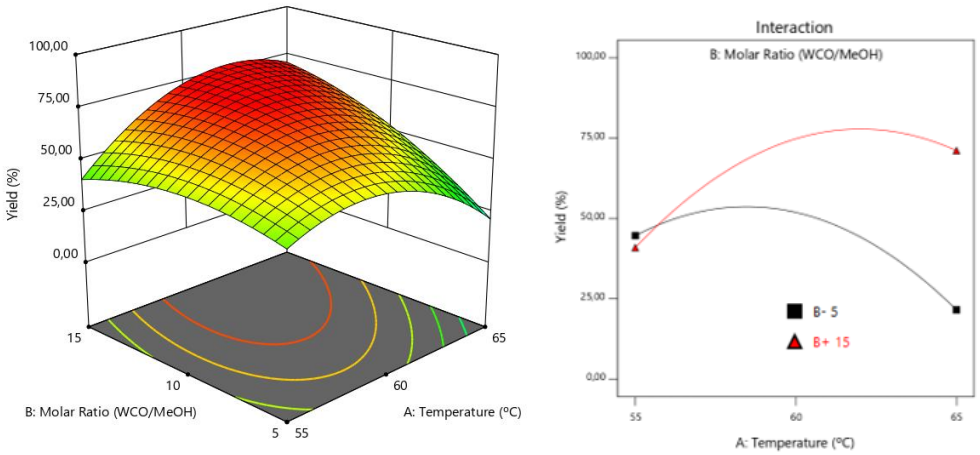

Figure 32. Response surface regarding the influence of temperature (A) and molar ratio WCO/MeOH (B) on the yield and the interaction plot of those variables.

Performing the analysis in a similar way to the one presented for the yield, it is possible to see that the response surface indicates that the variable A has a great influence on the FAME content results, since there is variation between the levels of the factors.

On the other hand, for variable B it is possible to verify that the response increases when the levels of factors vary. Thus, factors A and B have greater influence on yield response.

The interaction graph factors A and B shows two non-parallel lines representing the interaction between the factors to the studied response, that is, the effect caused by the change in the level of factor A in the response is dependent of the level of factor B and vice versa.

Figure 33 shows the response surface in relation to the influence of the variables: temperature (A) and catalyst dosage (C), and the interaction graph for these two variables.

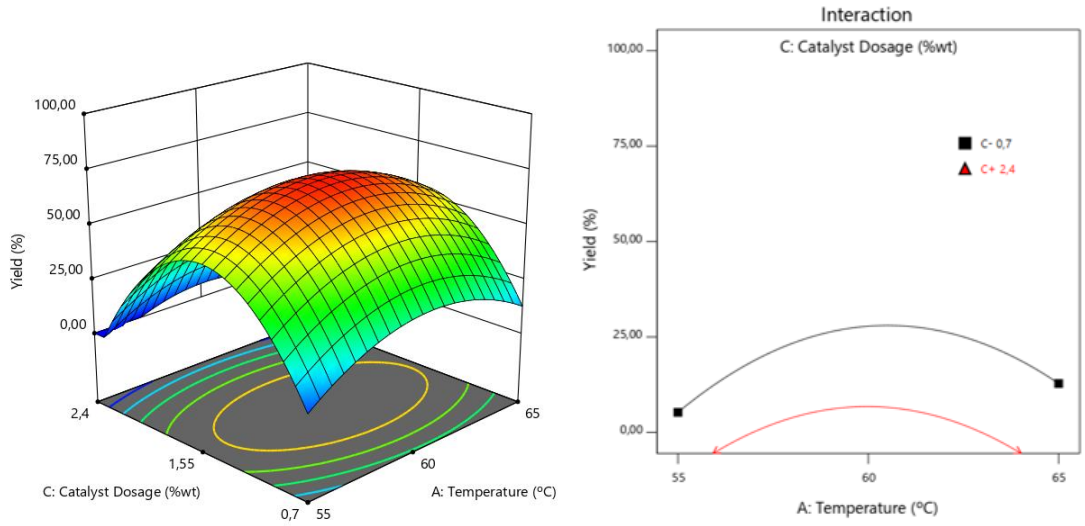

Figure 33. Response surface regarding the influence of temperature (A) and catalyst dosage (C) on the yield and the interaction plot of those variables.

The response surface indicates that variable A and C has a great influence on the yield results. Analysing the variation of the inclination in the straight lines in relation of the axis, it is also observed a great variation between the values obtained between the levels studied.

The interaction graph factors A and C shows two non-parallel lines representing the interaction between the factors to the studied response, that is, the effect caused by the change in the level of factor A in the response is dependent of the level of factor C, on the other hand the factor C depends on the factor A.

Figure 34 shows the response surface in relation to the influence of the variables: temperature (A) and incorporation of OA (D), and the interaction graph for these two variables.

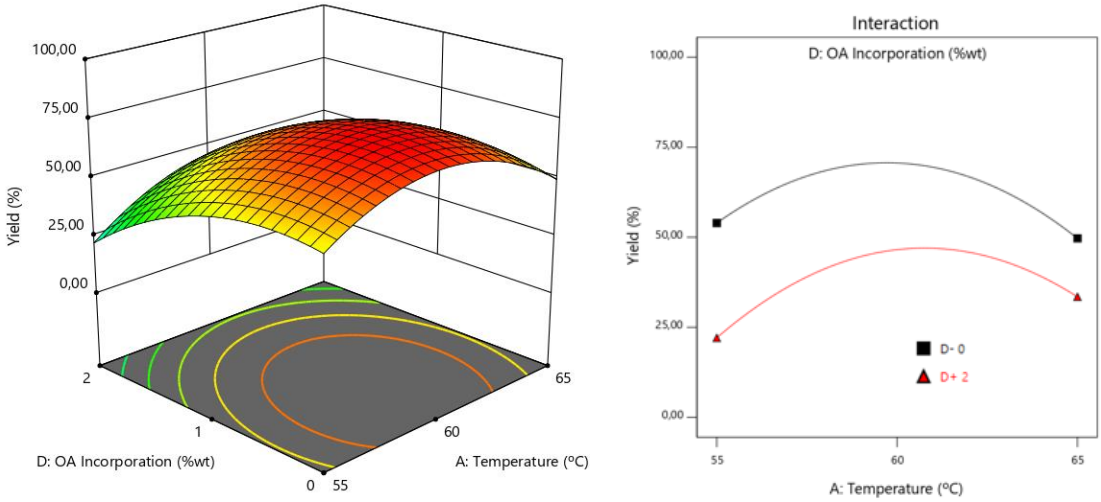

Figure 34. Response surface regarding the influence of temperature (A) and incorporation of oleic acid (D) on the yield and the interaction plot of those variables.

The response surface indicates that variable D has a great influence on the results. Thus, the d factor has a greater effect on the yield response than does the A factor. For the A factor, the yield response hardly changes along the A axis between levels.

The interaction graph factors A and D shows two non-parallel lines representing the interaction between the factors to the studied response, that is, the effect caused by the change in the level of factor A in the response is dependent of the level of factor D, on the other hand the factor D depends on the factor A.

Figure 35 shows the response surface in relation to the influence of the variables: molar ratio WCO/MeOH (B) and catalyst dosage (C), and the interaction graph for these two variables.

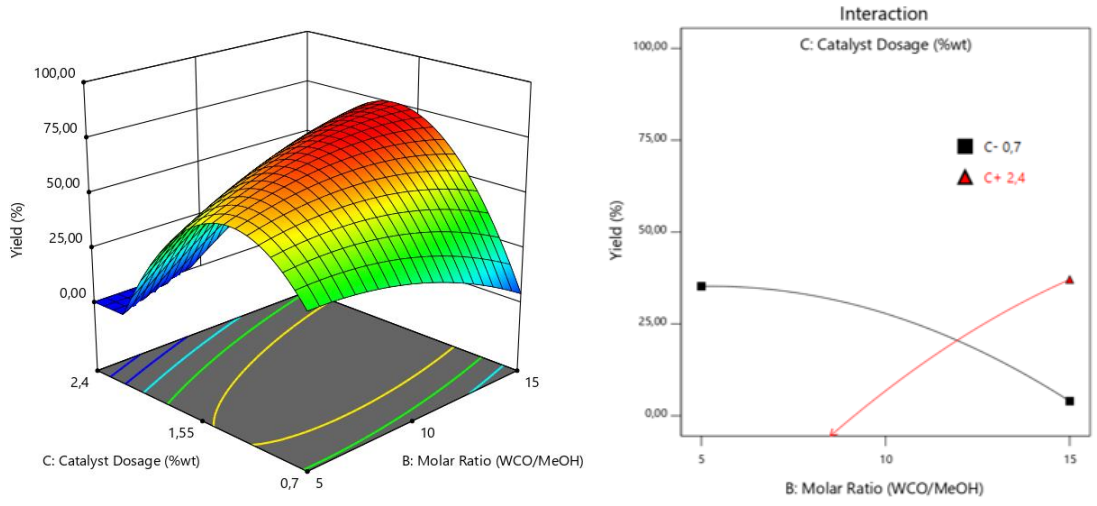

Figure 35. Response surface regarding the influence of molar ratio WCO/MeOH (B) and catalyst dosage (C) on the yield and the interaction plot of those variables.

The response surface indicates that variable B has a great influence on the yield results. Analysing the variation of the inclination in the straight lines in relation to the C axis, it is also observed a great variation between the values obtained between the levels studied.

The interaction graph factors B and C shows two non-parallel lines representing the interaction between the factors to the studied response, that is, the effect caused by the change in the level of factor B in the response is dependent of the level of factor C and vice versa.

Figure 36 shows the response surface in relation to the influence of the variables: molar ratio of WCO/MeOH (B) and incorporation of oleic acid (D) and the interaction graph for these two variables.

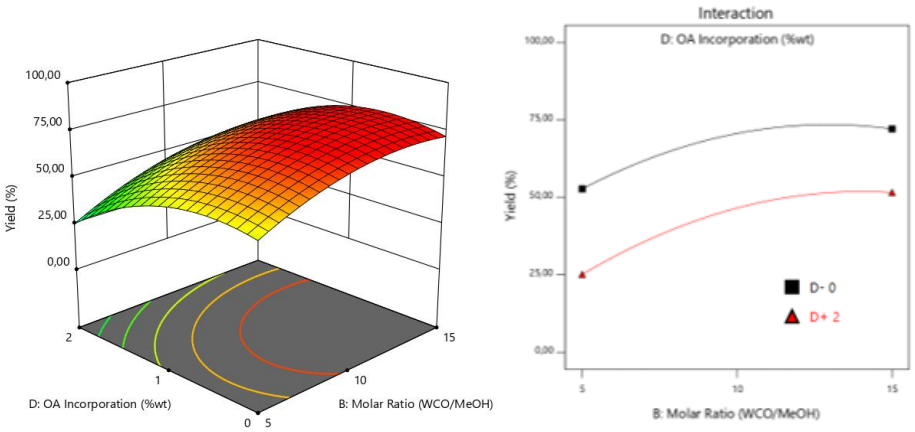

Figure 36. Response surface regarding the influence of molar ratio WCO/MeOH (B) and incorporation of oleic acid (D) on the yield and the interaction plot of those variables.

The response surface indicates that variable B has a great influence on the results. Thus, analysing factor D, a variation can also be observed. Factor D has a negative effect on yield, while factor B has a possible effect.

The interaction plot of factors B and D shows two lines practically parallel which represent the absence of interaction between the factors in the response, that is, the effect caused by the change in the factor B level in the response is independent of the factor level D and vice versa. It is confirmed the non-existence of this interaction by the analysis

of the p-value determined in ANOVA, where the interaction BD has no significance for the model developed.

Figure 37 shows the response surface in relation to the influence of the variables: catalyst dosage (C) and incorporation of oleic acid (D) and the interaction graph for these two variables.

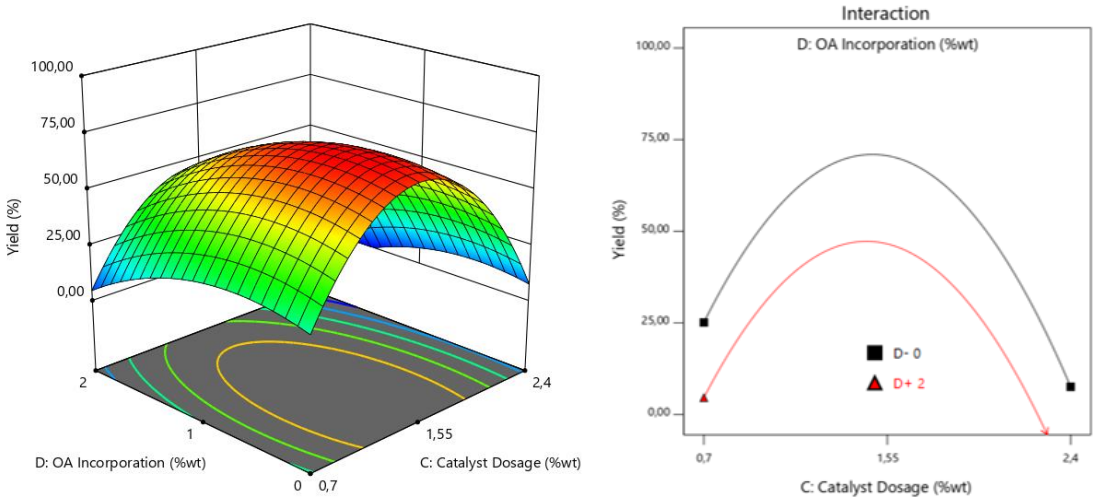

Figure 37. Response surface regarding the influence of catalyst dosage (C) and incorporation of oleic acid (D) on the Yield and the interaction plot of those variables.

The response surface indicates that variable C and D has a great influence on the Yield results. Analysing the variation of the inclination in the straight lines in relation of the axis, it is also observed a great variation between the values obtained between the levels studied.

The interaction graph factors C and D shows two non-parallel lines representing the interaction between the factors to the studied response, that is, the effect caused by the change in the level of factor C in the response is dependent of the level of factor D and vice versa.

5.3.2.8 Mathematical model for the Yield

Table 22 shows the coefficients determined for the mathematical model constructed through the regression of the experimental data corresponding to the acidity value response. From the calculated coefficients, it is possible to build the equation that best

fits the total factor studied. This model represents how the studied factors, and their interactions influence the acidity value response. The model equation is represented by Equation (13).

Table 22. Coefficients for yield.

Coded factor	Coefficient
Intercept	71.5
A	1.78
B	11.45
C	-10.53
D	-12.03
AB	13.32
AC	-2.00
AD	3.91
BC	27.09
BD	1.79
CD	-1.79
A^2	-18.79
B^2	-8.22
C^2	-54.27
D^2	-12.97

$$Y = 71.56 + 1.78A + 11.45B - 10.53C - 12.03D + 13.32AB - 2.00AC + 3.91AD + 27.09BC + 1.79BD - 1.79CD \pm 18.79A^2 - 8.22B^2 - 54.27C^2 - 12.97D^2 \quad (14)$$

In Equation (14) factors A, B and interactions AB, AD, BC, BD have a positive effect on the response, while factor C, D and other interactions have a negative effect.

5.3.2.9 Optimum conditions for the yield

For the studied conditions, factors, and their respective contents, it was possible to determine the best conditions to obtain the maximum yield from the waste cooking oil. The best conditions with coded and actual values are shown in Table 23.

Table 23. Best conditions for yield.

Factor	ID factor	Optimum value
A	Temperature	63ºC
B	Molar ratio WCO /MeOH	1:13 (mol/mol)
C	Catalyst Dosage	1.5 %
D	Incorporation of OA	0.5%

According to these conditions, to have a yield of 73.70%, an acidity value of 0.61 and a FAME content of 85.4% is required, for a confidence level of 95%.

6. CONCLUSIONS AND SUGGESTIONS OF FUTURE WORK

The main objective of this study was the production of biodiesel through the transesterification reaction of a simulated oil, from waste cooking oil and oleic acid, catalyzed by choline hydroxide.

The variation in the results was due to the fact that the ChOH catalyst is basic, and a neutralization reaction occurred when the catalyst was added at relatively small dosages, especially for artificially acidified oil samples. Therefore, the ChOH catalyst revealed high sensitivity towards the acidity of the oil.

The most relevant factors were the molar ratio between waste cooking oil and methanol, catalyst dosage and incorporation of oleic acid. For main responses: FAME content and yield. It was possible to define the ideal conditions that lead to the greatest possible FAME content and the highest possible yield. The optimal condition to obtain 85.4% FAME content and 73.7% of yield was estimated at 63ºC, molar ratio of 1:13, 1.5wt% of catalyst and 0.5wt% of OA incorporation.

These results indicate that this catalyst has a high potential in the production of biodiesel, as it leads to a high content of fatty acid methyl esters, even in small amounts of catalyst.

The experimental design allowed us to understand how each factor (temperature, molar ratio oil/methanol, catalyst dosage and incorporation of OA) influences the acidity value, the FAME content and the yield of the biodiesel samples obtained, when ChOH is used as a catalyst. Thus, it was possible to observe that the most relevant factors were the molar ratio WCO/MeOH, the dosage of the catalyst and the incorporation of OA for all responses (FAME content and yield).

The results obtained in this work are considered relevant for the application of basic catalysis in the transesterification reactions of mixtures of triacylglycerols derived from waste oils with high FFA content, since ChOH revealed excellent capacity for rapid transesterification.

As some results to produce biodiesel were not as satisfactory as expected, it would be necessary to carry out further studies on the influence of the incorporation of oleic acid in the production of biodiesel using ChOH as a catalyst:

- Study ChOH recovery to assess the number of reaction cycles in which a high FAME content can be achieved.
- Evaluate the quality of the biodiesel produced, determining its properties, for example: density, kinematic viscosity, and water content.

7. REFERENCES

[1] C. O. Hwai, Y. WeiTiong, H. H. Brandon, Y. G. Yong, M. M., I. Fattah, T. C. Cheng, M. A. Alam, H. VoonLee, A.S.Silitonga and T.M.IMahlia, *Recent advances in biodiesel production from agricultural products and microalgae using ionic liquids: Opportunities and challenges. Energy Conversion and Management, 113647. doi:10.1016/j.enconman.2020.113647,* 2020.

[2] M. Mohadesi, A. Gouran and A. Dehnavi, *Biodiesel production using low cost material as high effective catalyst in a microreactor. Energy. doi:10.1016/j.energy.2020.119671,* 2020.

[3] F. J. Deive, *Green Sustainable Process for Chemical and Environmental Engineering and Science, Ionic liquids for enzyme-catalyzed production of biodiesel.doi:10.1016/B978-0-12-817386-2.00002-0,* pp. 31-47, 2020.

[4] A. Gholami, F. Pourfayaz, A. Hajinezhad and M. Mohadesi, *Biodiesel production from Norouzak (Salvia leriifolia) oil using choline hydroxide catalyst in a microchannel reactor. Renewable Energy, S0960148119300576. doi:10.1016/j.renene.2019.01.057*, 2019.

[5] M. Gad and M. A. Ismail, *Effect of waste cooking oil biodiesel blending with gasoline and kerosene on diesel engine performance, emissions and combustion characteristics. Process Safety and Environmental Protection,S095758202031836X. doi:10.1016/j.psep.2020.10.040*, 2020.

[6] A. Tanweer, D. Mohammed, K. Pradeep, G. Belete, A. Samuel, N. Maniruddin e A. Muhammad, *Optimization of process variables for biodiesel production by transesterification of flaxseed oil and produced biodiesel characterizations. Renewable Energy, 139, 1272–1280. doi:10.1016/j.renene.2019.03.036,* 2019.

[7] M. Mofijur, S. Y. A. Siddiki, M. B. Ahmed, D. F, I. R. Fattah, H. C. Ong, M. Chowdhury and T. Mahlia, *Effect of nanocatalysts on the transesterification reaction of first, second and third generation biodiesel sources- A mini-review. Chemosphere, 128642. doi:10.1016/j.chemosphere.2020.128642*, 2020.

[8] K. Golmohammad, K. Kamran, R. Hamed, R. Mojtaba, H. Mehrdad and K. Mahmoud, *Experimental exergy analysis of transesterification in biodiesel production. Energy, 196, 117092. doi:10.1016/j.energy.2020.117092*, 2020.

[9] R. Morgana and O. W. Perez-Lopez, *FTIR spectroscopy analysis for monitoring biodiesel production by heterogeneous catalyst. Vibrational Spectroscopy, 105, 102990. doi:10.1016/j.vibspec.2019.102990*, 2019.

[10] A. S. Yusuff, A. O. Gbadamosi and L. T. Popoola, "Biodiesel production from transesterified waste cooking oil by zinc-modified anthill catalyst: Parametric optimization and biodiesel properties improvement.," *Jornal of Environmental Chemical Engineering*, vol. 9(2), 2021, https://doi.org/10.1016/j.jece.2020.104955.

[11] N. Gaurav, S. Sivasankari, G. Kiran, A. Ninawe and J. Selvin, *Utilization of bioresources for sustainable biofuels: A Review. Renewable and Sustainable Energy Reviews, 73, 205–214. doi:10.1016/j.rser.2017.01.070*, 2017.

[12] N. Manojkumar and Chandrasekaran, *Heterogeneous nanocatalysts for sustainable biodiesel production: A review,,Journal of Environmental Chemical Engineering, doi:https://doi.org/10.1016/j.jece.2020.104876*, 2020.

[13] M. Mumtaz, *Clean Energy for Sustainable Development, Biodiesel Production Through Chemical and Biochemical Transesterification, 465–485. doi:10.1016/B978-0-12-805423-9.00015-6*, 2017.

[14] A. Moina and Z. Sadaf, *A review of the feedstocks, catalysts, and intensification techniques for sustainable biodiesel production. Journal of Environmental Chemical Engineering,104523. doi:10.1016/j.jece.2020.104523*, 2020.

[15] C. TungChong, T. YuLoe, K. Y. Wong, V. Ashokkumar, S. ShiungLam, W. TongChong, A. Borrion, B. Tian and Jo-HanNg, *Biodiesel sustainability: The global impact of potential biodiesel production on the energy–water–food (EWF) nexus.https://doi.org/10.1016/j.eti.2021.101408*, 2021.

[16] R. R. d. O. P. Lima, *Estudo da Produção de Biodiesel por Transesterificação Usando Hidróxido de colina como Catalizador. Dissertação de Mestrado, Instituto Politécnico de Bragança*, 2020.

[17] X. Ma, F. Liu, Y. Helian, C. Li, Z. Wu, H. Li, H. Chu, Y. Wang, Y. Wang, W. Lu, M. Guo, M. Yu and S. Zhou, *Current application of MOFs based heterogeneous catalysts in catalyzing transesterification/esterification for biodiesel production: A review. https://doi.org/10.1016/j.enconman.2020.113760,* 2021.

[18] S. Soltani, U. Rashid, I. A.-R. Saud and A. N. Imededdine, *Recent progress in synthesis and surface functionalization of mesoporous acidic heterogeneous catalysts for esterification of free fatty acid feedstocks: A review. Energy Conversion and Management, S0196890416306203. doi:10.1016/j.enconman.2016.07.042,* 2016.

[19] D. Z. Troter, Z. B. Todorović, D. R. Đokić-Stojanović, O. S. Stamenković and V. B. Veljković, *Application of ionic liquids and deep eutectic solvents in biodiesel production: A review. Renewable and Sustainable Energy Reviews, 61, 473–500. doi:10.1016/j.rser.2016.04.011,* 2016.

[20] E. I. Abdalla, *Experimental studies for the thermo-physiochemical properties of Biodiesel and its blends and the performance of such fuels in a Compression Ignition Engine. Fuel, S0016236117313108. doi:10.1016/j.fuel.2017.10.064,* 2017.

[21] M. Athar and S. Zaidi, *A review of the feedstocks, catalysts, and intensification techniques for sustainable biodiesel production. Journal of Environmental Chemical Engineering, (), 104523–. doi:10.1016/j.jece.2020.104523,* 2020.

[22] L. G. Balu and S. S. Ganapati, *Choline based ionic liquids and their applications in organic transformation. Journal of Molecular Liquids, 227, 234–261. doi:10.1016/j.molliq.2016.11.136,* 2017.

[23] S. Phromphithak, P. Meepowpan, S. Shimpalee and N. Tippayawong, *Transesterification of palm oil into biodiesel using ChOH ionic liquid in a microwave heated continuous flow reactor. Renewable Energy, 154, 925–936. doi:10.1016/j.renene.2020.03.080,* 2020.

[24] Sahar, S. Sana, I. Javed, U. Inam, B. H. Nawaz, N. Shazia, Habib-ur-Rehman, N. Jan and I. Munawar, *Biodiesel production from waste cooking oil: An efficient*

technique to convert waste into biodiesel. Sustainable Cities and Society, 41, 220–226. doi:10.1016/j.scs.2018.05.037, 2018.

[25] S. Adeyinka, K. Aman, T. Jayati, P. Dinesh, P. Lok and A. Neeraj, *Synthesis and characterization of coal fly ash supported zinc oxide catalyst for biodiesel production using used cooking oil as feed*, pp. 302-314, 2021.

[26] F. Mingming, H. Jianglei, Y. Jing and Z. Pingbo, *Biodiesel production by transesterification catalyzed by an efficient choline ionic liquid catalyst. Applied Energy, 108, 333–339. doi:10.1016/j.apenergy.2013.03.063,* 2013.

[27] N. Azizi and M. Edrisi, *Biodegradable choline hydroxide promoted environmentally benign thiolysis of epoxides. Tetrahedron Letters, S0040403915304950. doi:10.1016/j.tetlet.2015.12.080,* 2015.

[28] d. H. Isabel, Y. Pérez and M. Fajardo, *Supported choline hydroxide (ionic liquid) on mesoporous silica as heterogeneous catalyst for Knoevenagel condensation reactions. Microporous and Mesoporous Materials, S1387181117308065. doi:10.1016/j.micromeso.2017.12.024,* 2017.

[29] Y. Lu, Q. Yangbo, Z. Yan, T. Cong and S. Jiangnan, *A continuous mode operation of bipolar membrane electrodialysis (BMED) for the production of high-pure choline hydroxide from choline chloride. Separation and Purification Technology, 233, 116054. doi:10.1016/j.seppur.2019.116054,* 2020.

[30] S. Phromphithak, P. Meepowpan, S. Shimpalee and N. Tippayawong, *Transesterification of palm oil into biodiesel using ChOH ionic liquid in a microwave heated continuous flow reactor. Renewable Energy, 154, 925–936. doi:10.1016/j.renene.2020.03.080,* 2020.

[31] A. C. C. Lima, *Evaluation of Alkaline Ionic Liquids for Catalysis of Biodiesel from Cooking Oil. Master's Thesis, Polytechnic Institute of Bragança, Portugal,* 2020.

[32] I. Belhaj, *Biodiesel production through esterification catalyzed by imidazolium based ionic liquids. Master's Thesis, Polytechnic Institute of Bragança,Portugal,* 2019.

[33] C. V. B. Meireles, *Processos químicos catalisados por líquidos iónicos para produção de ésteres metílicos de ácidos gordos. Dissertação de Mestrado, Instituto Politécnico de Bragança,Portugal,* 2018.

[34] F. F. Roman, *Biodiesel Production through Esterification Applying Ionic Liquids as Catalysts. Master's Thesis,Polytechnic Institute of Bragança, Portugal,* 2018.

[35] A. Tadevosyan, *Biodiesel Production through Ionic Liquid Catalysed Esterification. Master's Thesis, Polytechnic Institute of Bragança,Portugal,* 2017.

[36] I. Alimova, *Production of Biodiesel through Esterification Catalysed by Ionic Liquids. Master's Thesis, Polytechnic Institute of Bragança, Portugal,* 2016.

[37] H. O. R. Diniz, *Valorização de óleos alimentares usados através de processos de conversão em biodiesel catalisados por líquidos iónicos. Dissertação de Mestrado, Instituto Politécnico de Bragança, Portugal,* 2020.

[38] "EUROPEAN STANDARD 14103,Fat and oil derivatives - Fatty Acid Methyl Esters (FAME) - Determination of ester and linolenic acid methyl ester contents," February 10 2020. [Online]. Available: https://standards.iteh.ai/catalog/standards/sist/0b80f2a4-4b98-4797-9c4d-155b5d0567b6/sist-en-14103-2020#!. [Accessed 22 February 2021].

[39] M. Sarno and M. Iuliano, *Highly active and stable Fe 3 O 4 /Au nanoparticles supporting lipase catalyst for biodiesel production from waste tomato. Applied Surface Science, S0169433218310146. doi:10.1016/j.apsusc.2018.04.060,* 2018.

[40] Supelco, "Bulletin 907," [Online]. Available: https://www.sigmaaldrich.com/Graphics/Supelco/objects/8100/8046.pdf. [Accessed 28 February 2021].

[41] L. Vieira, R. Schennach and B. Gollas, "In situ PM-IRRAS of a glassy carbon electrode/deep eutectic solvent interface," *Physical Chemistry Chemical Physics,* vol. 17, no. 19, pp. 1287-12880 . doi:10.1039/C5CP00070J, 2015.

[42] M. A. Bezerra, R. E. Santelli, E. P. Oliveira, L. S. Villar and L. A. Escaleira, " Response surface methodology (RSM) as a tool for optimization in analytical chemistry.," vol. 5, no. 76, pp. 0-977, 2008. doi:10.1016/j.talanta.2008.05.019.

[43] R. Wasserstein and N. Lazar, "The ASA Statement on p-Values: Context, Process, and Purpose. The American Statistician," pp. 129-133, 9 June 2016.

[44] S. Almasi, G. Najafi and S. Jalili, "Biodiesel production from sour cherry kernel oil as novel feedstock using," *Biocatalysis and Agricultural Biotechnology,* p. 35, 2021.doi:10.1016/j.bcab.2021.102089 .

[45] G. K. Ghosh, A. Kotia, N. Kumar and S. Kumar, "Optimization and modeling of rheological characteristics for graphene-gear oil based nanolubricant using response surface methodology," *Physicochemical and Engineering Aspects,* vol. 630, 2021. https://doi.org/10.1016/j.colsurfa.2021.127605.

[46] C. Dougherty, "Introduction to Econometrics (second edition 2002, Oxford University Press, Oxford). Statistical Tables," 2002. [Online]. Available: https://home.ubalt.edu/ntsbarsh/business-stat/StatistialTables.pdf. [Accessed 24 10 2021].